Medicine

Sperm motility in mice with Oligo-astheno-teratozoospermia restored by in vivo injection and electroporation of naked mRNA

Reviewed Preprint

Published from the original preprint after peer review and assessment by eLife.

About eLife's process

Reviewed preprint version 1
February 28, 2024 (this version)

Posted to preprint server
December 14, 2023

Sent for peer review
December 12, 2023

Charline Vilpreux, Guillaume Martinez, Magali Court, Florence Appaix, Jean-Luc Duteyrat, Maxime Henry, Julien Vollaire, Camille Ayad, Altan Yavz, Lisa De Macedo, Geneviève Chevalier, Emeline Lambert, Sekou Ahmed Conte, Elsa Giordani, Véronique Josserand, Jacques Brocard, Coutton Charles, Bernard Verrier, Pierre F. Ray, Corinne Loeuillet, Christophe Arnoult, Jessica Escoffier

Université Grenoble Alpes, Inserm U1209, CNRS UMR 5309, Team Genetic, Epigenetic and Therapies of infertility, Institute for Advanced Biosciences 38 000 Grenoble, France • UM de Génétique Chromosomique, Hôpital Couple-Enfant, CHU Grenoble Alpes, Grenoble, France • Université Grenoble Alpes, Inserm U1209, CNRS UMR 5309, plateforme microcell, Institute for Advanced Biosciences 38 000 Grenoble, France • Université Claude Bernard Lyon 1, CNRS UAR3444, Inserm US8, ENS de Lyon, SFR Biosciences, Lyon 69007, France • Université Grenoble Alpes, Inserm U1209, CNRS UMR 5309, plateforme Optimal, Institute for Advanced Biosciences 38 000 Grenoble, France • Université Claude Bernard Lyon 1 – Laboratoire de Biologie Tissulaire et d'Ingénierie Thérapeutique, UMR 5305, Université Lyon 1, CNRS, IBCP, Lyon, France • UM GI-DPI, CHU Grenoble Alpes, Grenoble, France

Abstract

Oligo-astheno-teratozoospermia (OAT), a recurent cause of male infertility, is the most frequent disorder of spermatogenesis with a probable genetic cause. Patients and mice bearing mutations in the *ARMC2* gene have a decreased sperm concentration, and individual sperm show multiple morphological defects and a lack of motility – a canonical OAT phenotype. Intra Cellular Sperm Injection (ICSI) is required to treat such a condition but it has limited efficacy and was associated with a small increase in birth defects. Consequently, new targeted treatments are needed to restore spermatogenesis. Here, a combination of *in vivo* injection and electroporation of capped and poly-A-tailed naked mRNA is tested as a strategy to treat *ARMC2*-related infertility in mouse. mRNAs coding for several reporter genes are tested and the efficiency and the kinetic of expression are assessed using *in vivo* and *in vitro* 2D and 3D imaging experiments. We show that mRNA-coded reporter proteins are detected for up to 3 weeks mostly in germ cells, making the use of mRNA possible to treat infertility. We compare these results with those obtained with a more conventional DNA plasmid vector. In contrast, the use of the non-integrative plasmid Enhanced Episomal Vector (EEV) shows low and transient expression in spermatogenic cells. Consequently, injection and electroporation of naked mRNA-*Armc2* into the testes of *Armc2*-deficient males were performed and we show the presence of normal and motile sperm in the epididymis. This study shows for the first time that mRNA-*Armc2* efficiently restores spermatogenesis and opens new paths for male infertility treatment.

Ethics statement

All procedures involving animals were performed in line with the French guidelines for the use of live animals in scientific investigations. The study protocol was approved by the local ethics committee (ComEth Grenoble #318) and received governmental authorization (ministerial agreement #38109-2022072716142778).

eLife assessment

This potentially **useful** study reports a new method for restoring sperm motility. Strengths are in the methodology being developed, but the conclusions require additional experimental support. The authors provide **inadequate** evidence for the success of the method or its mechanism.

Introduction

Worldwide, 10-15% of couples (or 70 million) face infertility [1]. Infertility is thus a major public health issue presenting significant medical, scientific and economic challenges (a multibillion € annual market) [2]. A significant proportion of infertility is due to altered gametogenesis, where the sperm and eggs produced are incompatible with fertilization and/or embryonic development. Approximately 40% of cases of infertility involve a male factor, either exclusively, or associated with a female deficiency.

Male gametogenesis, or spermatogenesis, is a highly complex physiological process which can be split into three successive steps: proliferation (mitosis of spermatogonia), reduction of the number of chromosomes (meiosis of spermatocytes), and spermatid differentiation (spermiogenesis). The whole process involves several thousands of genes, of which a large part are expressed almost exclusively in the testes [3]. Because of this multiplicity of genes, spermatogenesis is strongly affected by genetic factors [3], with most severe disorders likely to be of genetic origin.

For patients with severe infertility, only assisted reproductive technologies (ARTs) – such as Intra Cytoplasmic Sperm Injection (ICSI) – can efficiently overcome the problems faced. However, there are some concerns surrounding the risks associated with this technique; statistical analyses of birth records has shown a real risk of birth defects associated with ICSI [4]. To overcome these drawbacks, a number of experimental strategies have been proposed to bypass ARTs and restore spermatogenesis, including gene therapy [5–8].

Gene therapy consists of introducing a DNA sequence into the genome to compensate for a defective gene. It can thus rescue production of a missing protein, and is now widely applied both in research and for the treatment of human diseases. Given the genetic basis of male infertility, the first strategy tested to overcome spermatogenic failure associated with monogenic diseases was delivery of an intact gene to deficient germ cells. Gene therapy works efficiently in germ cells, and numerous publications have shown that conventional plasmids can be transferred into spermatogonia in several species with a high success rate, allowing their transcription in all cells of the germinal lineage [5–8]. Most experiments were performed in mouse models, delivering DNA constructs into living mouse germ cells by testis electroporation after microinjection of a DNA-containing solution into the seminiferous tubules. Using this method, it was possible to rescue meiosis and fertility in mouse models of infertility [5, 8]. However, the genetic changes induced are transmitted to any descendants. Consequently, gene therapy cannot be used

to treat infertility in humans, as for both ethical reasons and to avoid any eugenic deviations, transmissible changes are illegal in humans in most countries. Moreover, genetic modification of germ cell lines presents multiple biological risks, including that of inducing cancer [9, 10]. Gene therapies have thus raised both ethical controversy and long-term safety issues.

For these reasons, we decided to test an alternative strategy to DNA transfection based on the use of naked mRNA. Thanks to this small change, there should be no risk of genomic insertion, and thus there is no question of heritable alterations. The first part of this study presents a complete characterization of the protein expression patterns obtained following transfection of naked mRNA coding for reporter genes into the testes of mice.

Among infertility disorders, oligo-astheno-teratozoospermia (OAT) is the most frequent; it is likely to be of genetic origin. Spermatocytograms for OAT patients show a decrease in sperm concentration, multiple morphological defects and defective motility. Because of these combined defects, patients are infertile and can only conceive by ICSI. The aim of this work was 1/ to perform a full characterization of the efficiency of naked mRNA to express proteins, using reporter genes, and 2/ to apply the protocol to a preclinical mouse model of OAT. Patients and mice carrying mutations in the *ARMC2* gene present a canonical OAT phenotype and are completely infertile. The preclinical *Armc2* deficient (*Armc2* KO) mouse model is therefore a valuable model to assess whether *in vivo* injection of naked mRNA combined with electroporation can restore sperm spermatogenesis. We chose this model for several reasons: first, it is an easy model to implement. Armc2 KO mice are sterile and all sperm exhibit short, thick or coiled flagella [13]. As a result, 100% of sperm are completely immobile, thus it should be easy to determine the efficacy of the technique by measuring sperm motility with a CASA system. Second, the Armc2 gene codes for an 867-amino acid protein and this large size represents a challenge for expression in the testis following electroporation.

To determine the efficacy of naked mRNA transfection as a method to achieve protein expression in the testes, we assessed the level of transcription of reporter proteins after mRNA injection compared to the injection of a non-integrating plasmid, the Enhanced Episomal Vector (EEV). EEV is a vector derived from Epstein-Barr virus, it includes an EBV Ori and the EBNA1 protein. It does not integrate or modify the host genome. Replication of this vector is synchronized with host cell division [11, 12].

In the present in vivo work, we injected and electroporated three distinct mRNAs coding for the reporter proteins green fluorescent protein (GFP), luciferase (Luc) and mCherry, and an EEV episome vector containing the sequences coding for both GFP and luciferase reporter proteins. We first characterized and validated the method of injection via the rete testis followed by electroporation in adult males. Next, we compared the kinetics and patterns of expression of the electroporated mRNAs and EEV by several methods, including whole testis imaging, in vivo bioluminescence imaging and tissue clearing.

Then we used a preclinical mouse model of OAT to test the mRNA transfection protocol, with the aim of restoring fertility. Three- and 5-weeks after injection and electroporation of *Armc2*-mRNA into the testes of *Armc2* KO mice, we identified normal motile sperm cells in the epididymis.

Materiel and methods

Animals

All procedures involving animals were performed in line with the French guidelines for the use of live animals in scientific investigations. The study protocol was approved by the local ethics committee (ComEth Grenoble #318) and received governmental authorization (ministerial

agreement #38109-2022072716142778).

The animals used were B6D2 F1 hybrid (♀ C57BL/6JRj crossed with ♂ DBA/2, Janvier laboratories;france) adult male mice aged between 8 and 25 weeks, and the *Armc2* KO mouse strain obtained by CRISPR-Cas9, as described in Coutton et al. 2019. Experiments were carried out on wild type (WT) or *Armc2* KO adult male mice aged between 8 and 15 weeks.

Chemicals and reagents

Fast Green (FG) (F7258 – 25 g), phosphate buffered saline (PBS, D853 7-500 mL), hematoxylin (GH5316 – 500 mL), eosin (HT110216 – 500 mL), terbutanol (471712 – 100 mL), Histodenz (D2158 – 100 g), sorbitol (S1876 – 100 g) and urea (U5128 – 500 g) were purchased from Sigma Aldrich (Saint Louis, MI, USA). Schorr staining solution was obtained from Merck (XXX). Mfel HF (R35895) and RNase-free DNase I (M03035) were obtained from New England Biolabs (Ipswich, MA, USA). Paraformaldehyde (PFA, 15710) was obtained from Electron Microscopy Science (Hatfield, PA, USA). Ketamine and xylazine were obtained from Centravet (Dinan, France). Fluorescent i-particles NIRFiP-180 were obtained from Adjuvatis (Lyon, France). CleanCap AG, CleanCAp *EGFP*-mRNA and CleanCap *Luciferase*-mRNA were obtained from Tebubio (Le Perray en Yvelines, france).

Plasmids

All plasmids were amplified by bacterial transformation (E. coli, EC0112; Thermo Fisher, Waltham, MA, USA). After expansion, plasmids were purified with a NucleoBond Xtra Midi kit (740410-50; Macherey-Nagel, Düren, Germany). DNA pellets were solubilized in (DNAse- and RNAse-free) milliQ water.

Non-integrative episome EEV *CAGs-GFP-T2A-Luciferase*

The EEV *CAGs-GFP-T2A-Luciferase* (EEV604A-2) used for *in vivo* testis microinjection and electroporation was obtained from System Biosciences (Palo Alto, CA, USA). This episome contains the cDNA sequences of Green Fluorescent Protein (GFP) and luciferase, under the control of a CAGs promoter (**supp Fig 1**). After purification, the EEV *CAGs-GFP-T2A-Luciferase* plasmid concentration was adjusted to 9 µg μL^{-1}. Prior to injection, 3.3 µL of this plasmid solution was mixed with 1 µL 0.5% Fast Green and 5.7 µL sterile PBS to obtain a final EEV concentration of 3 µg mL^{-1}.

mCherry plasmid

The was obtained from Dr. Conti's lab at UCSF. This plasmid contains the cDNA sequence of *mCherry* under the control of CMV and T7 promoters (**supp Fig 1**). After amplification and purification, the final plasmid concentration was adjusted to 9 µg μL^{-1}.

Plasmid EEV-*Armc2-GFP*

The EEV-*Armc2-GFP* plasmid used for *in vivo* testes microinjection and electroporation was obtained from Trilink (San Diego, USA). This non-integrative episome contains the cDNA sequences of *Armc2* and the Green Fluorescent Protein (GFP) genes under the control of a strong CAGs promoter (**Fig 1** supplementary).

After amplification and purification, the final plasmid concentration was adjusted to 9 µg μL^{-1}. Prior to injection, 3.3 µL of this plasmid solution was mixed with 1 µL of 0.5% Fast Green and 5.7 µL of sterile PBS to obtain a final EEV concentration of 3 µg μL^{-1}.

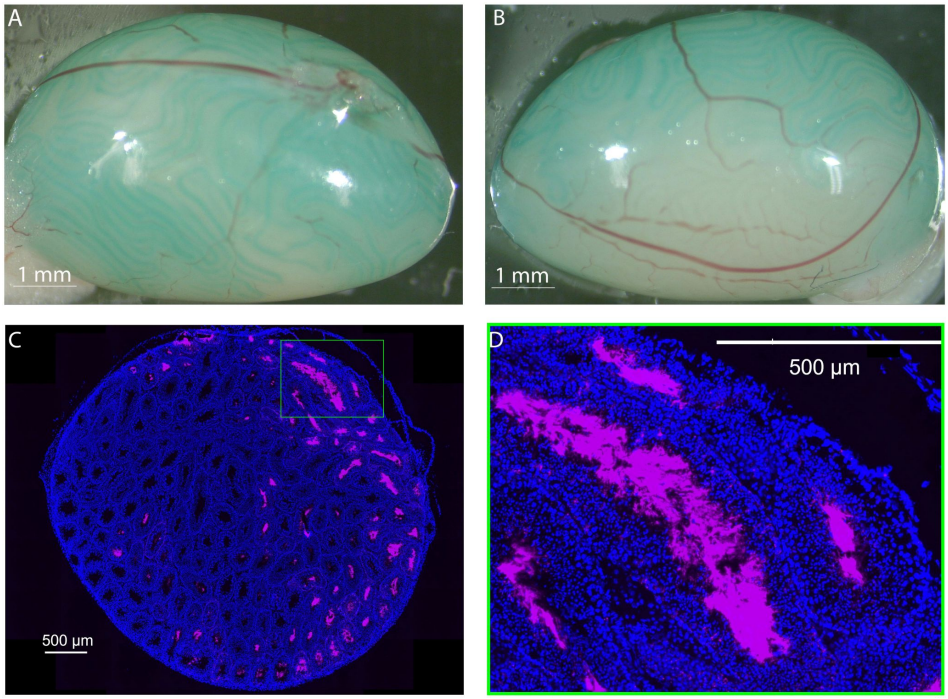

Figure 1

Distribution of I-particles NIRFIP-180 in testis injected via the rete testis route.

(A) A solution containing 0.05% Fast Green and 1% fluorescent i-particles NIRFiP-180 was prepared, 10 µL was injected into the seminiferous tubules of adult males, through the *rete testes* and its efferent channels. Injection was performed at constant pressure under a binocular microscope. The progression of filling of the seminiferous tubules was monitored thanks to the Fast Green (B). The testes were only filled to 2/3 capacity in order to prevent damage to the tissue. (C) Representative distribution of fluorescent i-particles NIRFiP-180 in a whole cross-section of an injected testis. Nuclei were counterstained with DAPI (blue emission) to reveal tubules. (D) Enlargement of a seminiferous tubule showing particles localized inside the lumens of the tubules. Scales bars: 1 mm and 500 mm.

Armc2-mRNA

Armc2-mRNA used for in vivo testes microinjection and electroporation was obtained from Trilink (San Diego, USA). The commercial *Armc2*-mRNA has an AG CleanCap, a poly A tail of 120 adenosines and 3 HA FLAG. The main challenge with mRNA-based therapies is mRNA stability. To improve mRNA stability in vivo and avoid its degradation by ribonucleases, optimization techniques were implemented. Thus, the used mRNA had codon optimization, a polyA tail and a CleanCap. To verify germ the efficiency of cell transfection, an *EGFP*-mRNA was injected together with the *Armc2*-mRNA. During the injection, the concentration of *EGFP*-mRNA and *Armc2*-mRNA were 300 ng μL^{-1} each.

mcherry-mRNA transcription *in vitro*

The circular *mCherry* plasmid was linearized using the restriction enzyme Mfel HF at 37 °C for 1 h. The pm-*mCherry* was then extracted and purified with the DNA Clean and Concentrator-25 ^{TM} kit (D4033; Zymo Research, Irvine, CA, USA). The pm-*mCherry* was subsequently transcribed in vitro using the T7-FlashScribe kit (C-ASF3507; Tebubio, Le Perray en Yvelines, France). The mRNA was capped with a clean cap (CleanCap AG, Tebubio), and a poly A tail (C-PAP5104H; Tebubio) was added before purification using the NucleoSpin RNA Clean Up kit (740948-50; Macherey-Nagel). Prior to injection, *mcherry*-mRNA was mixed with Fast Green to obtain a final concentration of 300 ng mL^{-1} (0.05% FG, PBS).

Agarose gel electrophoresis of the Episomal Vector EEV and mRNA-mCherry

Before loading on a pre-stained (Gel Green) 1.5% agarose gel, the EEV-plasmid and mRNA were mixed with a loading dye (Promega Blue Orange G1904). An aliquot of each sample (500 ng) was loaded into each well and electrophoresis was performed for 30 min at 100 V at room temperature (RT). A DNA size marker (Gene ruler, Thermo Scientific, SM1331) was used to assess molecular weight. Gel images were acquired using a ChemiDoc XRS+ (BIORAD).

In vivo microinjection and electroporation of testes

Electroporation was conducted as previously described [7]. Briefly, male mice B6D2, *Armc2* +/+ or *Armc2* -/-, depending the experimental conditions, were anesthetized with ketamine/xylazine solution (100mg mL^{-1} and 10 mg mL^{-1} respectively). The testes were pulled out of the abdominal cavity or scrotum. Under a binocular microscope and using microcapillaries pipettes (FemtoTip II ®, Eppendorf, Montesson, France), 10 mL DNA (3 mg mL^{-1} -0.05% FG) or mRNA (300 ng mL^{-1} -0.05% FG) was injected into the seminiferous tubules through the *rete testis* applying constant pressure (microinjector, Femto Jet 4i). Two series of 8 square electric pulses (25 V for 50 ms) were applied to the testis using tweezer-type electrodes linked to an electroporator (Gemini, BTX, Holliston, USA). The testes were then replaced in the abdominal cavity, and the abdominal wall and skin were sutured. For each animal, the left testis was injected and electroporated with the different nucleic acids (mRNA, EEV), whereas the right testis was injected with a control solution (PBS, 0.5% FG) as a control. Both testes were electroporated.

Flash Freezing and Fluorescence Analysis of testes

Depending on the experimental condition, 1-, 3- or 7-days post injection, the testes were collected and washed for 5 min in PBS. Then, they were embedded in Peel-A-Way Cryomolds filled with OCT (OCT Mounting media VWR BDH CHEMICALS). The samples were flash frozen in a 100% isopentane solution (Carlo ERBA), pre-cooled with liquid nitrogen. Once frozen, they were cut into 20-µm sections using a cryostat. The cryostat sections were then fixed with 4% PFA-PBS for 10 min at 4 °C and counterstained with 1.8 mM DAPI (nuclear stain) before observation using an Axioscan

Z1 slide scanner or a confocal AxioObserver Z1 multiparameter microscope LSM710 NLO – LIVE7 – Confocor3 . The fluorescence of the different reporter proteins was detected using appropriate filters for DAPI, GFP, Texas Red (for mCherry), and Cy7 (for the Fluorescent i-particles NIRFiP-180).

Tissue collection and histological analysis

For histological analysis, treated and control B6D2 testes were fixed by immersion in 4% paraformaldehyde (PFA) for 14 h. They were then embedded in paraffin before cutting into 5-µm sections using a microtome (Leica biosystems). After deparaffination, the sections were stained with hematoxylin and eosin. Stained sections were digitized at ×20 magnification using an axioscan Z1-slide scanner (Zeiss, Germany). Spermatogenesis was assessed by measuring the area of seminiferous tubules (μm^2) and the cross sections of round tubules ((n > 35 tubules per testis section; n= 5 testis sections per condition). Statistical significance of differences was determined using a Student t-test.

Ex vivo Fluorescence Analysis

To analyze the expression of the reporter proteins GFP and mCherry in seminiferous tubules, whole testes were examined under an inverted microscope (Olympus, CKX53). Exogenous fluorescence was detected using filters for GFP and Texas Red.

Harris-Shorr sperm Analysis

Sperm cells were collected from the caudae epididymides of mice (Control, injected with EEV-*GFP*, *GFP*-mRNA, or *Armc2*-mRNA). They were allowed to swim for 10 min at 37 °C in 1 mL M2 media. Sperm cells were centrifuged at 500 x g, washed once with PBS, and fixed in PBS/4% paraformaldehyde for 1 min at RT. After washing with 1 mL acetate ammonia (100 mM), the sperm cell suspensions were spotted onto 0.1% poly L-lysine precoated slides (Thermo Scientific) and left to dry. Harris–Schorr staining was then performed according to the WHO protocol [14], and at least 100 sperm cells were analyzed per animal.

Whole Testis Optical clearing and 3D image reconstructions

Optical clearing (adapted from uDISCO and Fast 3D clear protocols)

Adult mice were euthanized by cervical dislocation and transcardial perfusion with 1X PBS (Sigma-Aldrich). The testes were extracted and fixed for two days at 4 °C in 4% PFA (Electron Microscopy Sciences). Samples were then washed with PBS for at least two days. Mouse testes were subsequently dehydrated in graded series of tert-butanol solutions (Sigma-Aldrich) at 35 °C as follows: 30% overnight (O/N), 50% for 24 h, 70% for 10 h, 80% O/N, 90% for 10 h, 96% O/N, and 100% for 10 h. The testes were cleared in clearing solution (96 % Histodenz,2% Sorbitol, 20 % Ure) for 2 days. Then, nuclei were stained with 3.6 mM DAPI (20% DMSO; 2% Triton, 1% BSA) for 2 days. Finally, the testes were then conserved in the clearing solution at 4°C until the microscopy observation. All these steps were carried out under agitation and protected from light.

3D tissue Imaging

The optically-cleared mouse testes were imaged on a lightsheet fluorescence microscope (Blaze, Miltenyi Biotec, Germany), using a 4x NA 0.35 MI PLAN objective protected by a dipping cap for organic solvents, with an overall working distance of 15 mm. Acquisitions on the horizontal plane were obtained with a fixed lightsheet thickness of 3.9 µm at both 488 nm and 561 nm with no overlap between horizontal planes. Voxel resolution x = 1.21; y = 1.21; z = 2 µm. 3D reconstructions were created using Imaris software (Oxford Instruments plc, Tubney Woods, Abingdon, Oxon OX13 5QX, UK).

Cellular image analysis

The optically-cleared mouse testes were imaged using a 'ConfoBright' system which is a unique adaptive confocal microscope (Nikon A1R MP, Nikon Europe B.V., The Netherlands) equipped with a deformable mirror module (AOS-micro, AlpAO, Montbonnot, France) for the correction of geometrical aberrations. Indeed, the deep confocal imaging of the cleared 3D sample requires long distance objectives and immersion media of different refractive index, resulting in optical aberrations. Images were acquired using Adaptive Optics optimization with an apo LWD 40x/1.15 water immersion objective (WD 600 µm) and a 10x/0.45 objective. FIJI software was used to process and analyze images and Imaris software for the 3D reconstructions.

Bioluminescence imaging

In vivo Bioluminescence imaging was performed at several time points after *in vivo Luciferase* -mRNA or EEV-*GFP-luciferase* injection and electroporation (n = 5 mice per condition). Ten minutes before imaging, mice received an intraperitoneal injection of 150 µg g^{-1} of D-luciferin (Promega), and were then anesthetized (isoflurane 4% for induction and 1.5% for maintenance) before placing in the optical imaging system (IVIS Lumina III, PerkinElmer). *In vivo* bioluminescence signals were measured in selected regions of interest (injected testes) and were expressed as mean photons per second (mean ± SEM). Background bioluminescence was measured on images from control mice. When the *in vivo* bioluminescence signal was no longer detectable, testes were collected and immersed in a luciferin solution for a few minutes before performing *ex vivo* imaging to confirm the absence of signal.

Sperm motility

The cauda epididymis was dilacerated in 1 mL of M2 medium (Sigma-Aldrich, l'Isle d'Abeau, France) and spermatozoa were allowed to swim out for 10 min at 37 °C. Motility of the spermatozoa was evaluated with an Olympus microscope and Computer Aided Sperm Analysis (CASA) (CEROS II apparatus; Hamilton Thorne).

Western blot

Western blotting was performed on HEK-293T cells (ATCC, Manassas, VA, USA) transfected with EEV-*Armc2* or *Armc2*-mRNA. Cells were transfected using JetPrime (Polyplus, 101000027) for DNA and JetMessenger (Polyplus, 101000056) for mRNA vectors, both according to the supplier's recommendations. After 48 h, the cells were washed with PBS and scraped off before centrifuging at 4 °C, 1500 RPM for 5 min. The cell pellet was then resuspended in lysis buffer (Thermo Scientific, 87787) supplemented with an EDTA-free cocktail of protease inhibitors (Roche, 11836170001). The suspension was stirred at 4 °C for 2 h, and then centrifuged at 16,000 x g at 4 °C for 10 min. The protein content of the supernatant was estimated (QuantiPro™ BCA Assay kit; Sigma-Aldrich QPBCA) before adding 5X Laemmli + 5% β-mercaptoethanol and heating at 95 °C for 10 min. For the Western blot, 30 µg of proteins were deposited on a ready-made Bis-Tris gel 12 % (ThermoFisher). After transfer, the PVDF membrane was blocked with 5% milk in Tris-Buffered Saline solution containing 0.1% Tween 20 (TTBS) before immunodetection. The anti HA antibody (Cat. No. 11867423001, Sigma Aldrich) was diluted in TTBS at 1/5000. After incubation with secondary antibodies (AP136P, Sigma Aldrich, 1:10,000 in TTBS), binding was revealed with an enhanced chemiluminescence detection kit (ECL plus, Amercontrol Biosciences). Membranes were imaged on a ChemiDoc™ system (Bio-Rad).

Immunofluorescence

Immunofluorescence analysis of dissociated testicular cells was performed as follows. After collection, the tunica albuginea was removed from the testes. Then the tissue was mechanically digested with 18G needles. Once washed with PBS, the testicular cells were placed in a dissociation

medium (25 mL RPMI and 25 mg collagenase type V) for 20 min at 37 °C. After filtration (100 mM filter) and centrifugation (5 min at 200 x g) the pellets were resuspended in PBS before centrifugation once again. The pellet was then fixed in 1 mL PFA 4% for 5 min. Then 10 mL of ammonium acetate (0.1 M) was added. Finally, 2 mL of medium was spread on a slide. Testicular cells were permeabilized with 0.1% PBS-Triton X-100 for 20 min at room temperature. Slides were then blocked in 10% BSA with PBS-Tween 0.1% for 30 min before incubating overnight at 4 °C with primary antibodies anti-rabbit *ARMC2* (HPA053696, Sigma Aldrich, 1:50) and anti-guinea pig tubulin (AA345, Swiss Institute of Bioinformatics, 1:100) diluted in PBS-Tween 0.1% – 5% BSA. Slides were washed with PBS before incubating for 1 h with secondary antibodies (for tubulin: A-11073, Thermo Fischer Scientific, 1/500; for ARMC2: A-11036, Thermo Fischer Scientific, 1:1000). Samples were counterstained with DAPI and mounted with DAKO mounting media (Life Technology). Fluorescence images were acquired under a confocal microscope (Zeiss) fitted with a 63× oil immersion objective. Images were analyzed with ZEN lite software (Zeiss).

Statistical analyses

Statistical analyses were performed using SigmaPlot (version 10; Systat Software, Inc., San Jose, CA). To account for sample variability between animals, a paired t-test and Wilcoxon test were used. Data are displayed as mean ± SEM. P values of *≤0.05, **≤0.01, or ***≤0.001 were considered to represent statistically significant differences.

Results

1. *In vivo* microinjection and electroporation of mouse testes

Two routes have been described for microinjection of DNA into the testes: direct injection through the *tunica albuginea,* or injection into the lumen of the seminiferous tubules via the *rete testis*. We chose the *rete testis* route and evaluated the efficacy of the microinjection protocol, in particular as we wished to better characterize the diffusion of the injected solution in the volume of the testis, as we were unable to find any information on this parameter in the literature. The efficacy of microinjection *via rete testis* was assessed using fluorescent i-particles NIRFiP-180, and by measuring their diffusion in testis cross sections examined by microscopy 3 days post-injection (**Fig 1**). To avoid lesions due to overfilling, the injection was controlled by measuring the expansion of the staining of the peripheral seminiferous tubules during the injection. Injections were stopped when the testes were filled to 2/3 of their capacity (**fig 1** A-B). In testis cross sections, the fluorescent i-particles NIRFiP-180 were heterogeneously distributed, and mainly observed in seminiferous tubules located in the peripheral region of the testes, with fewer particles present in the center of the testes (**Fig 1 C-D**). Moreover, no fluorescent i-particles NIRFiP-180 were visible in the peritubular space. These results indicated that microinjection through the *rete testis* did not produce a homogenous distribution of the particles throughout the seminiferous tubules. Nevertheless, the seminiferous tubules remained intact, as no signal was observed in the peritubular space (**Fig 1C-D**).

Next, we assessed the overall safety of the *rete testis* microinjection and electroporation of mRNA and EEV into testes. The safety of the protocol was evaluated by comparing macroscopic and microscopic anatomies of control (injected with control solution, PBS, 0.05% FG), and treated testes (injected either with EEV-*GFP* (PBS, 0.05% FG) or *GFP*-mRNA (PBS, 0.05 % FG)). Three days post-injection, the testes were first observed under a binocular microscope to identify possible macroscopic degeneration of the seminiferous tubules (**Fig 2A**1 and 2B1). Degenerations appear as pearly white lesions at the surface of the testis as illustrated in **Supp Fig 1** following over electroporation. With the protocol used, no such lesions were observed. Next, the testes were measured and weighted. No differences were observed between control and treated testes (**Fig 2** A2, A3, B2, B3), Then, microscopic differences were sought by histological analysis of 5-µm sections (**Fig 2C**). No difference was observed between the control condition and EEV-*GFP* or

GFP-mRNA on the full cross sections (**Fig 2** C1, C2, C3). Next, we observed all the different testicular cells, including spermatogonia, spermatocytes, Sertoli cells, round spermatids and epididymal sperm cells (**Fig 2D** 1, D2, D3) in each condition. The layered structure of germ cells was respected in all cases. Analysis of the histological sections revealed no differences in the tubules area of the testes injected either with EEV-*GFP* or *GFP*-mRNA (**Fig 2E**). Finally, Harris-Shorr staining of the epididymal sperm cells showed no morphological defects (**Fig 2F**). Taken together, these results suggest that *in vivo* microinjection and electroporation of EEV or mRNA is safe.

2. Analysis of EEV-*GFP* and *GFP*-mRNA testicular expression by whole testis imaging

After validating the injection method, we compared the kinetics of GFP expression for mRNA and EEV. To do so, we injected and electroporated one testis of129 adult B6D2 mice with EEV-*GFP* and of 65 mice with *GFP*-mRNA. At 0, 1, 7, 15, 21-, 28-, 35-42 and 49-days post-injection, the whole testes were observed under an inverted microscope. The exogenous fluorescence was directly visible at the surface of the testes when illuminated with light at the appropriate wavelength (**Fig 3** and **4**). These observations revealed no testicular lesions at any post-injection time (**Fig 3** .A1-H1 and 4A1-F1). In addition, both *GFP*-mRNA and EEV-*GFP* induced GFP expression in the testes (**Fig 3A** 2-H2 and 4A2-F2). It is worth noting that both vectors induced GFP expression from the very first day. However, the durations of expression were different. For EEV, GFP fluorescence was still observable on day 42 for 100% of samples, and 56% of samples were positive on day 49, indicating that expression lasted around 1.5 months (**Fig 4G**). In contrast, for mRNA, 100% of testes were labelled on day 21, but none showed any fluorescence on day 28 (**Fig 4G**). Thus, EEV transfection allowed a considerably longer duration of expression than mRNA. (**Fig 3** and **4**). In addition to differences in duration of expression, the GFP expression patterns were clearly different: mRNA produced a large, diffuse pattern, highlighting the shape of the seminiferous tubules; EEV-*GFP* produced a punctiform pattern (**Fig 3B** and **4B**.) These results suggest that *GFP*- mRNA and EEV-*GFP* targeted different testicular cell types, or that there were differences in terms of efficiency of transfection.

3. Kinetics of EEV and mRNA expression assessed by *in vivo* imaging

To further assess and compare the kinetics of expression of the two vectors, we expressed exogenous luciferase in the testis using EEV or mRNA and observed the level of luciferase by *in vivo* bioluminescence imaging. For EEV, we took advantage of the fact that the EEV plasmids contains the DNA sequence of the luciferase protein (CAGs-GFP-T2A-Luciferase) in addition to the DNA sequence of the GFP fluorescent protein (**Fig supp 2**). For mRNA, we injected commercial naked *luciferase*-mRNA into the *rete testis* according to the same protocol as used for *GFP*-mRNA. For this set of experiments, we injected the EEV-*GFP-Luc* and *luciferase*-mRNA into the testes of 6 adult mice on day 0. Importantly, we injected a similar number of copies of mRNA and EEV. The testes were imaged *in vivo* to detect bioluminescence expression, on day 1 and weekly until disappearance of the signal, no more than 120 days post-injection (**Fig 5**). For EEV-*GFP-Luciferase*, the bioluminescence induced by transfection was detected from day 1. After a rapid decrease in signal intensity over the first 3 weeks, a weak but constant signal remained detectable for 3 months, then faded away (**Fig 5** A1-A2). For *Luciferase*-mRNA, expression was also detected from day 1. The bioluminescence decreased gradually over 3 weeks, becoming undetectable thereafter (**Fig 5B** 1-B2). These results are consistent with our previous results (**Fig 3**) and confirm that EEV allows a longer expression of exogenous protein within the testis. Overall, our results indicated stronger expression for mRNA than for EEV, but with expression decreasing rapidly over-time, and almost no remaining signal after 3 weeks. In contrast, residual expression was detectable for several months with EEV.

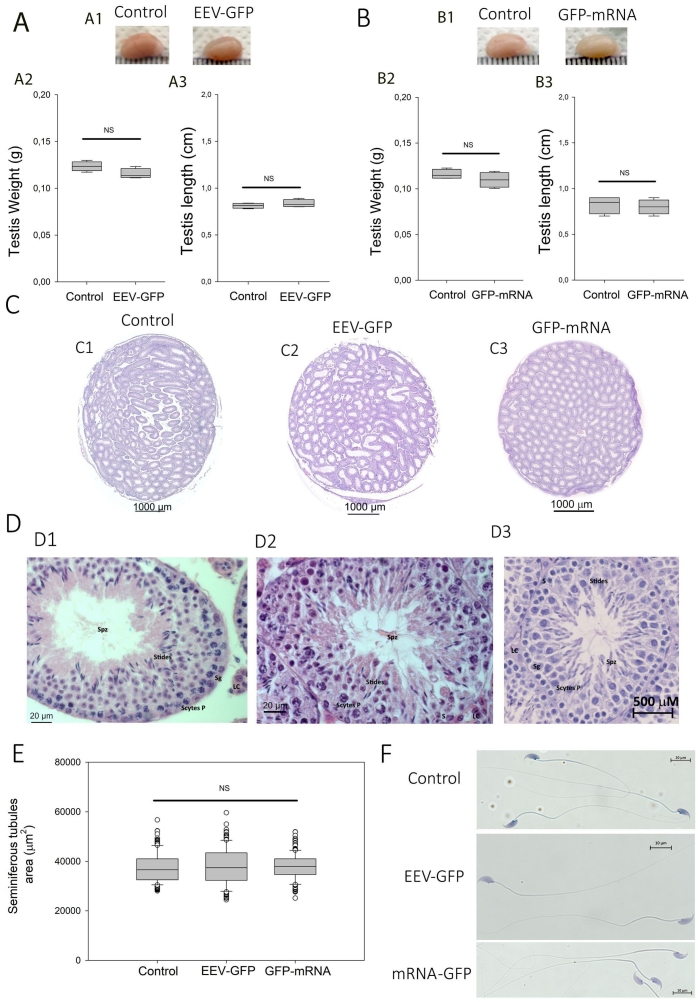

Figure 2

In vivo injection and electroporation do not alter the morphological structure of the testes, seminiferous tubules, or sperm cells.

(A, B) Testicular morphology was not affected by *in vivo* injection and electroporation of EEV-*GFP* (A) or *GFP*-mRNA (B). Controls corresponds to contralateral testes injected/electroporated with control solution (PBS, 0.05% FG). (A1, B1) comparison of the testicular morphology of adult testes injected with nucleic acid vectors or control solutions. (A2, B2) Comparison of testicular weight and (A3, B3) testicular length on day 7 after injection/electroporation. Data are represented as a box plot median (n=4 for each condition). A Wilcoxon matched pairs test was used to assess the significance of any differences in testis weights and lengths, and p values of ≤0.05 were considered statistically significant.
(C) Intact testicular structure after *in vivo* injection and electroporation with EEV-*GFP* and *GFP*-mRNA. Comparison of testicular cross section structures. Testes paraffin sections were stained with eosin/hematoxylin and observed by light microscopy (20X magnification). (C1) Control, (C2) EEV-*GFP* injected and (C3) *GFP*-mRNA injected. Scales bars: 1000 µm.
(D) Seminiferous tubule structures are not affected by *in vivo* injection and electroporation with EEV-*GFP* and *GFP*-mRNA. Enlargement of cross sections showing the fine structure of a seminiferous tubule for control (D1), EEV-*GFP* (D2) and *GFP*-mRNA (D3). In each tubule the different layers of spermatogenic cells are indicated, Sertoli cells (S), Spermatogonia (Sg), Spermatocytes (Scytes), rounds Spermatids (Stids) and sperm cells (Spz), Leydig cells (L). Scales bars: 500 and 20 µm.
(E) The area of seminiferous tubules is not affected by *in vivo* injection and electroporation with EEV-*GFP* and *GFP*-mRNA. Comparison of the seminiferous tubule diameter after injection of nucleic acid vectors or control solutions. Data are represented as a box plot median. The areas of seminiferous tubules (μm^2) were measured for round cross sections of $n > 35$ tubules per testis section (n= 5 testis sections per condition). Statistical significance was verified using a Student *t*-test.
(F) Injection/electroporation do not impact epididymal sperm cells. Representative sperm observed by light microscopy on day 7 after injection/electroporation with Control solution, EEV-*GFP*, or *GFP*-mRNA. Scale bars: 10 µm.

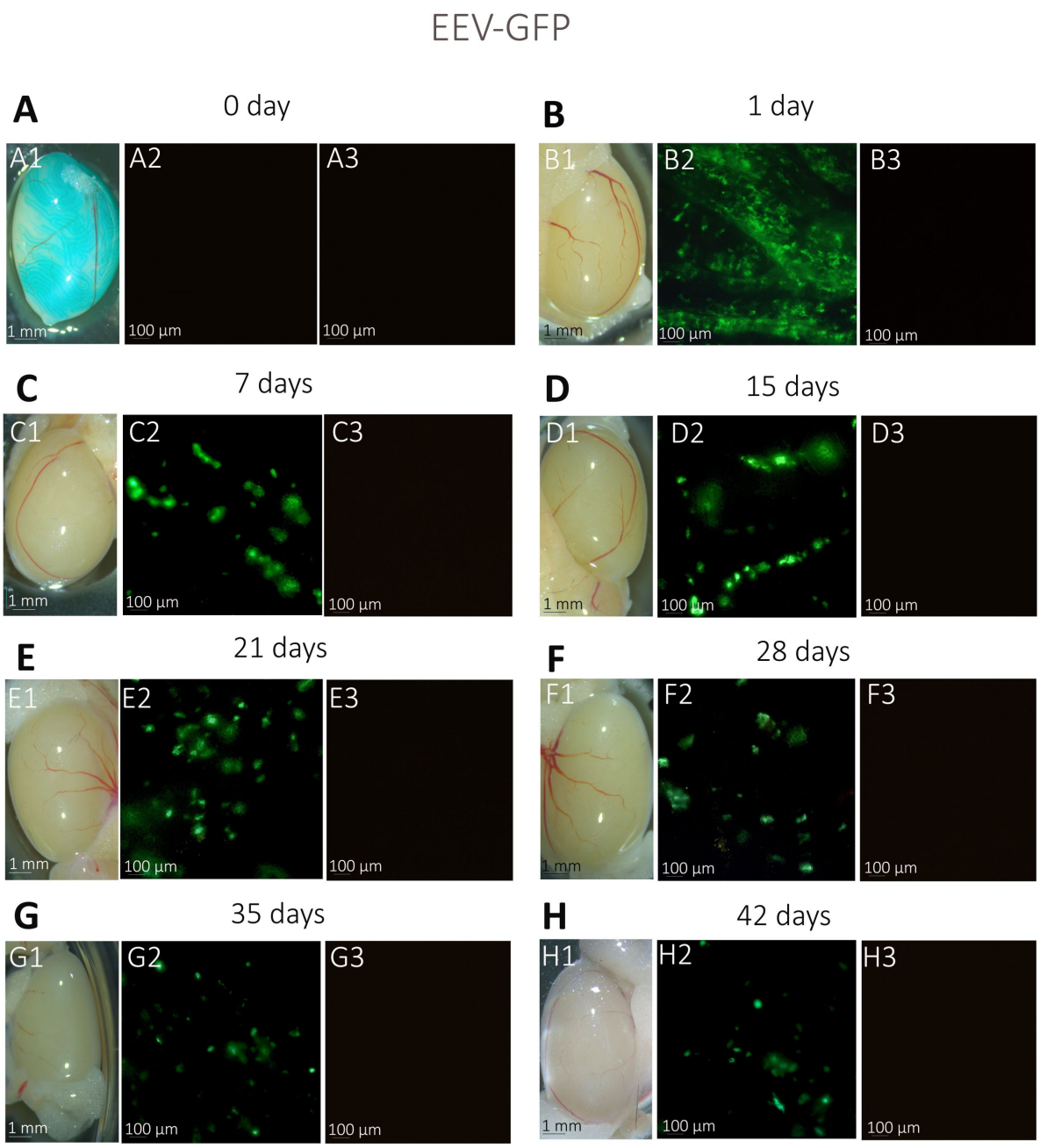

Figure 3

Kinetics of EEV-GFP expression following *in vivo* injection/electroporation: whole testicular expression

(A1-H1) Whole-mount testes on days 0, 1, 7, 14, 21, 28, 35 and 42 after *in vivo* injection/ electroporation with EEV-*GFP*. (A2-H2) Under fluorescence observation, GFP expression was detectable in transfected testes from 12-week-old B6D2 mice. (C3-H3) Insets show the absence of autofluorescence in non-transfected control testes. (4X magnification). The GFP expression presented a punctiform pattern in seminiferous tubules and was detected from 1 day to 42 days. Scales bars: 1 mm and 100 µm.

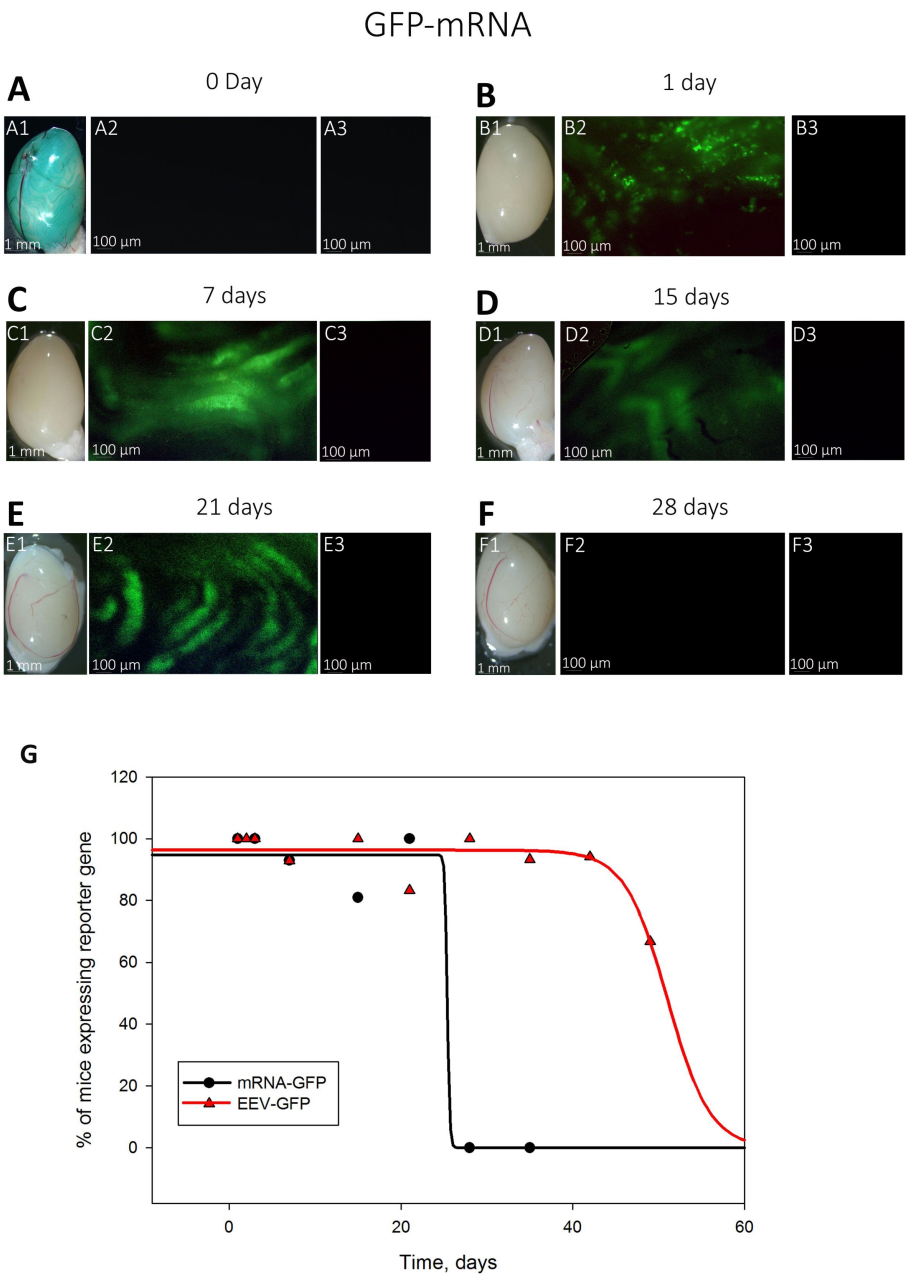

Figure 4

Kinetics of *GFP*-mRNA expression following *in vivo* injection/electroporation: whole testicular expression

(A1-F1) Whole-mount testes on days 0, 1, 7, 14, 21, and 28 after *in vivo* injection/ electroporation with *GFP*-mRNA. (A2-F2) Under fluorescence observation, GFP expression was detectable in transfected testes from 12-week-old B6D2 mice. (A3-F3) Insets show the absence of autofluorescence in non-transfected control testes. (4X magnification). The GFP expression presented a continuous pattern in seminiferous tubules and was detected from 1 day to 21 days. Scale bars: 1 mm and 100 µm.

(G) Comparison of number of injected mice exhibiting reporter gene expression. Mice injected with *GFP*-mRNA exhibited GFP expression from day 1 to day 21. Mice injected with EEV-GFP exhibited GFP expression from day 1 to 49 days. (for EEV-GFP n=11 on day 1; n=13 on day 2; n=10 on day 3; n=14 on day 7; n= 5 on day 10; n= 12 on day 15; n=11 on day 21; n= 12 on day 28; n=15 on day 35; n=17 on day 42 and n=9 on day 49) ; (for *GFP*-mRNA n=3 on day 1; n=4 on day 3; n=15 on day 7; n= 21 on day 15; n=15 on day 21 and n= 5 on day 28).

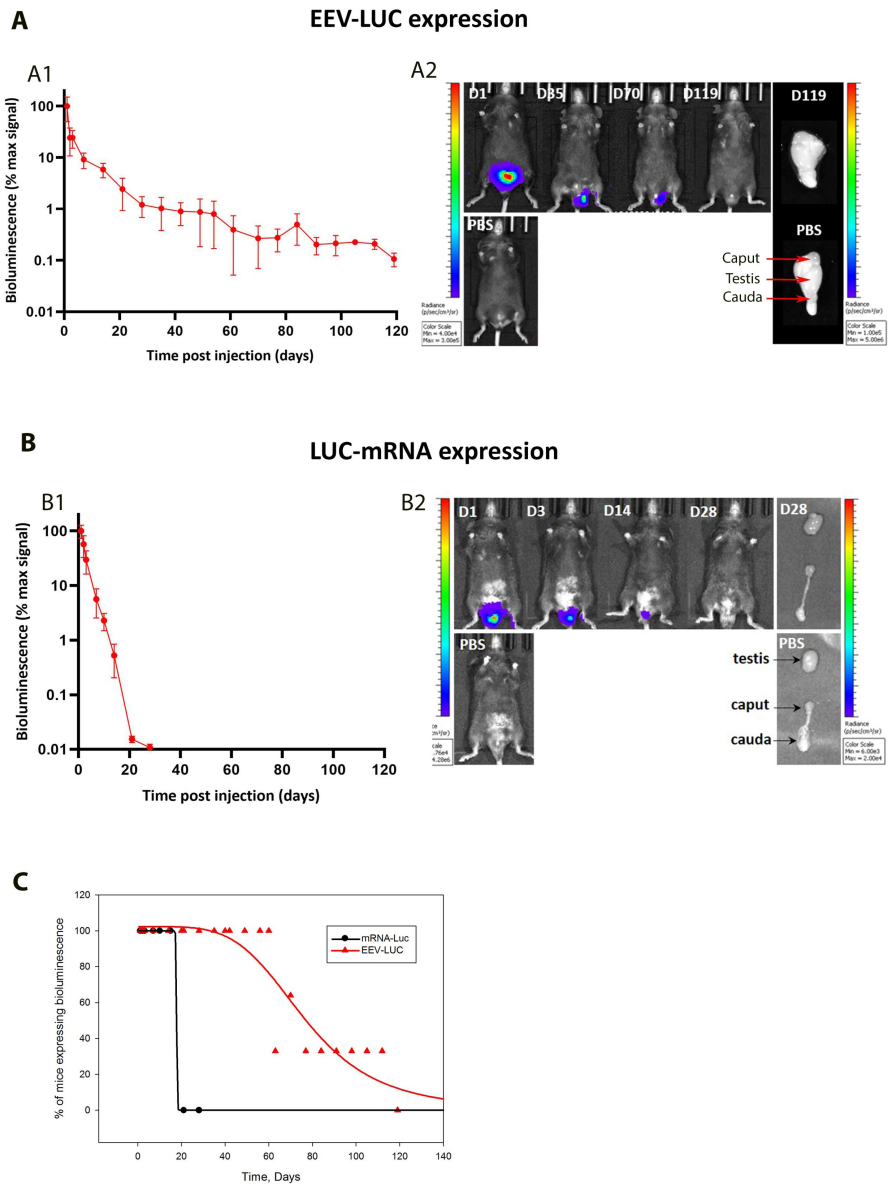

Figure 5

Kinetics of EEV and mRNA expression by *in vivo* bioluminescence imaging.

(A) *In vivo* bioluminescence imaging quantification of luciferase expression over time following injection/electroporation of EEV-*GFP-luc*. (A1): EEV-*GFP-Luc* was injected into the testes and electroporated on day 0. Bioluminescence signal was quantified at several time points. Results are expressed as the percentage of the maximal signal (mean ± SEM; n=5 mice up to D2; n=4 from D3 to D28; n=3 from D35 to D98 and n=3 from D105 to D119). (A2) *In vivo* bioluminescence images of a representative mouse at several time points after administering EEV-*GFP-LUC* or PBS, and ex vivo bioluminescence images of testes after 119 days.
(B) *In vivo* bioluminescence imaging quantification of luciferase expression over time induced by injection/electroporation of *LUC*-mRNA. (B1) *LUC*-mRNA was injected into the testes and electroporated on day 0. Bioluminescence signal was quantified in the whole testis at several time points. Results are expressed as the percentage of the maximal signal (mean ± SEM; n = 5 mice). (B2): *In vivo* bioluminescence images of a representative mouse at several time points after administering *LUC*-mRNA or PBS, and *ex vivo* bioluminescence images of caput, testes, and cauda after 28 days.
(C) Decay over time of the number of mice expressing reporter genes. Mice were injected on day 0 with *LUC*-mRNA or EEV-*GFP-LUC* and the number of mice showing bioluminescence in the testis was counted at different time points, from day 1 to day 119. For EEV-GFP: n=13 at D1; n=13 at D2; n=4 from D3 to D28; n=3 from D35 to D98 and n=3 from D105 to D119. For mRNA-Luc: n = 5 mice for all time points.

4. Assessing testicular and cellular *GFP*-mRNA expression using whole testicle optical clearing, light sheet microscopy, and 3D-microscopic reconstructions

To better characterize the spatial distribution of *GFP*-mRNA expression in the testis, we performed whole testicular optical clearing. On day 0, we injected and electroporated 6 testes with *GFP*-mRNA. On day 1, we harvested the testes, cleared them with a modified optical clearing protocol (see Methods). After complete clearing (**Fig 6 A**), we observed the testes under a light sheet microscope and performed 3D reconstruction (video 1, 2 and **Fig 6** BC). From this 3D reconstruction, we determined the volume of testis stained with GFP. The testis was sliced into 500 stacks, and the volume occupied by GFP staining was estimated by measuring the GFP-positive area in each stack and multiplying it by the thickness of the stack (10 µm). Measurements were possible only for the first 250 stacks due to optical problems with the last 250 stacks. To overcome this problem, and acquire information for the whole testis, the sample was turned by 180° and the measures repeated. A total GFP-stained surface of 0.51 mm^3 and 0.23 mm^3 was determined for face 1 and face 2, respectively. The corresponding total volume for the 250 stacks was measured as 60 mm^3, therefore 0.81% and 0.24% of the testis volume was transfected for face 1 and face 2 respectively (**Fig 6** BC).

5. Assessing GFP cellular expression using whole testicle optical clearing and confocal microscopy

Because the GFP fluorescence patterns were different for the two nucleic vectors when observed under the inverted microscope (**Fig 3**), we wondered whether the same cell types were targeted in both cases. To address this question, the whole optical cleared testes from EEV-*GFP* and *GFP*-mRNA-transfected mice were observed under a confocal microscope. The different cell types were identified based on their positions within the seminiferous tubule, their cellular shape and their nuclear morphology – revealed by nuclear staining. For instance, Sertoli cells have an oval to elongated nucleus and the cytoplasm presents a complex shape (“tombstone” pattern) along the basement membrane [15]. Round spermatids have small, round and compact nuclei with a nucleole and are localized between the spermatocytes and elongated spermatids [16]. For EEV-*GFP*, on day 1 post injection and electroporation, a strong punctiform green fluorescence was visible inside the seminiferous tubules (**Fig 7 A**). Based on the different morphological criteria, this fluorescent signal was detected in spermatocytes, round spermatids and Sertoli cells (**Fig 7** BC). On day 7, the GFP signal induced by EEV-*GFP* was reduced and only isolated signals in a few seminiferous tubules (1 per 11 tubules) were observed (**Fig 7 D**). These signals were associated only with Sertoli cells (**Fig 7 E**).

For the mRNA vector, on day 1 and day 7 post-injection and electroporation, an intense fluorescence was observed in all the germ cells in the seminiferous tubules (**Fig 8**). At the cellular level, this fluorescent signal was associated with Sertoli cells, spermatogonia, spermatocytes, round spermatids, elongated spermatids, and sperm cells to similar extents for both post-injection times (**Fig 8 B, D**). In contrast to what was observed with EEV on day 7, no reduction in the number of fluorescent seminiferous tubules was noted when using *GFP*-mRNA, with 8 out of 10 tubules stained (**Fig 8C**).

6. Expression of naked *mcherry*-mRNA in testis following electroporation

Heterologous expression is well known to depend on the protein studied, we therefore tested the same reporter proteins to compare the mRNA and EEV vectors in the experiments presented above. Apart from the bioluminescence experiments with luciferase, we compared only GFP protein expression. To validate and confirm the capacity of naked mRNA to safely express proteins

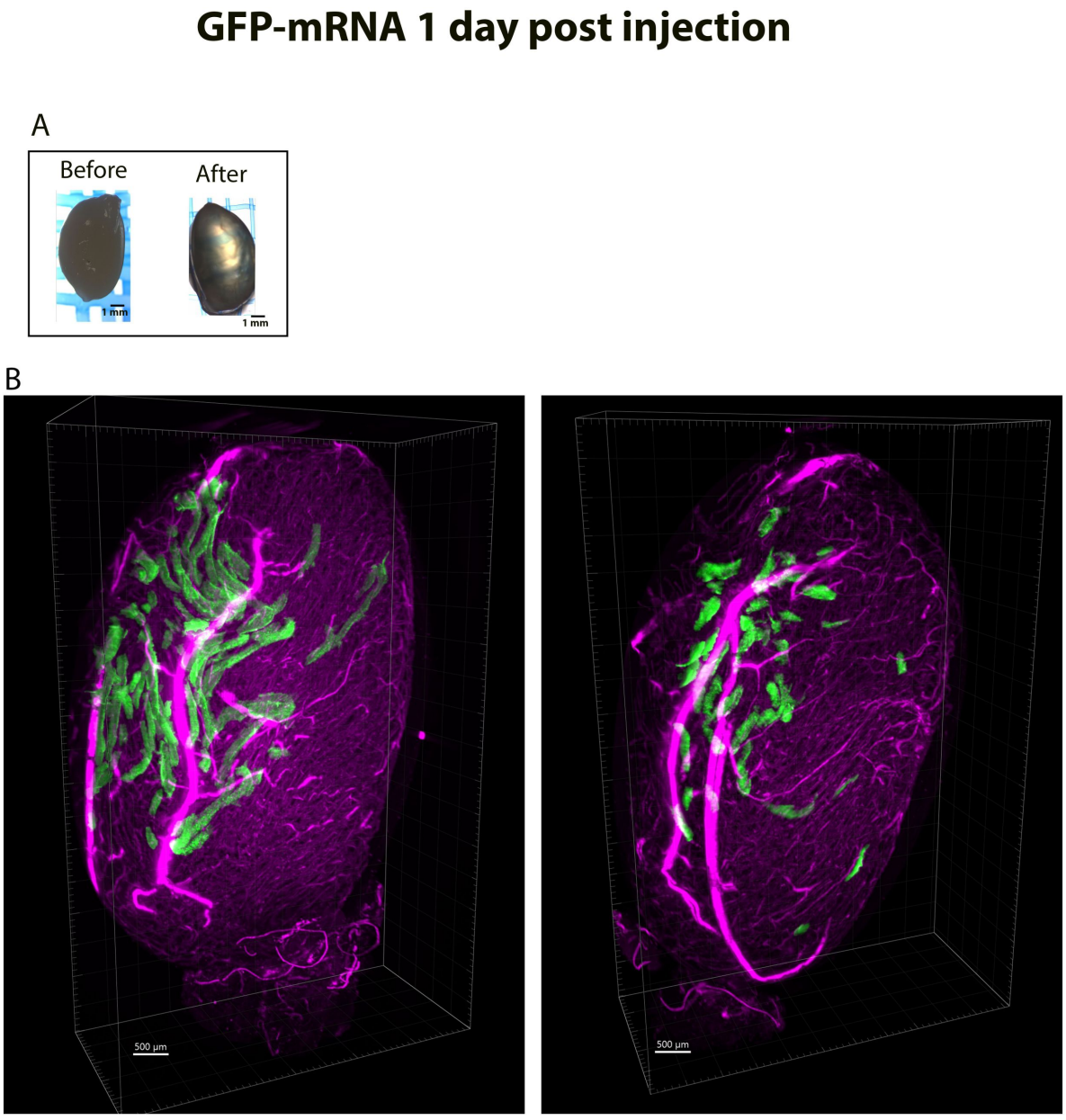

Figure 6.

Testicular and cellular *GFP*-mRNA expression measured on optically cleared testis after 3D image reconstructions from light sheet microscopy acquisitions.

Testes were injected/electroporated with *GFP*-mRNA on day 0. On day 1, whole testes were fixed and subjected to optical clearing. (A) Testes were observed before and after optical clearing on a binocular microscope. The right image shows the transparency of the testis after complete clearing, revealing the blue mesh throughout the organ. (B) The internal structure of a cleared testis was 3D reconstructed after lightsheet microscopy image acquisition. The reconstruction was possible only for a half testis due to light penetration constraints. Two opposing faces of the same testis are presented, allowing the distribution of GFP fluorescence throughout the seminiferous tubules to be measured. Pink fluorescence corresponds to the autofluorescence of interstitial cells located around the seminiferous tubules. Scale bars A: 1 mm and B:500 mm.

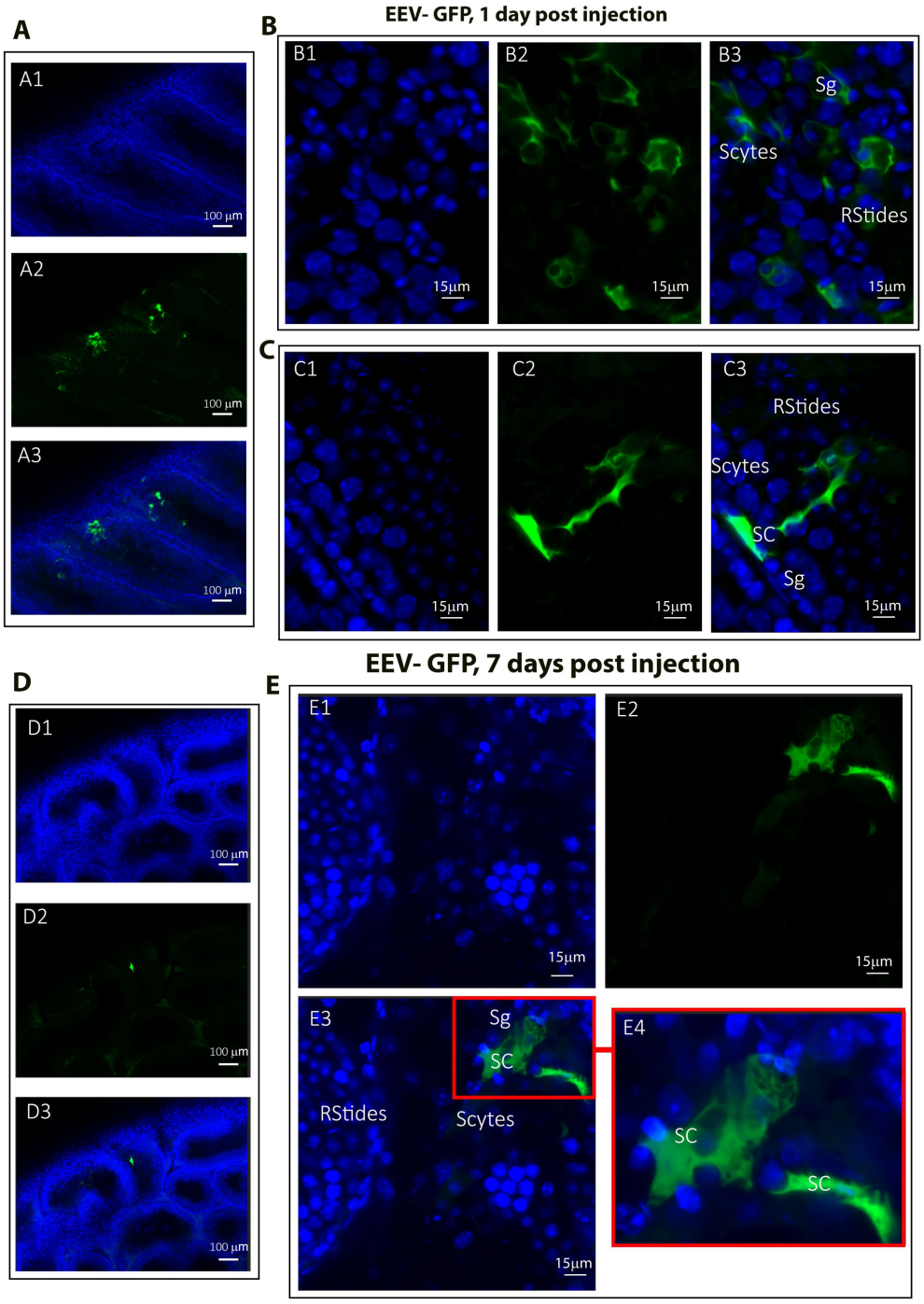

Figure 7.

Cellular expression of EEV-*GFP* following *in vivo* injection/ electroporation.

Testes were injected/electroporated with EEV-*GFP* on day 0. On day 1 and on day 7, whole testes were fixed and subjected to optical clearing. Cleared tested were observed by fluorescence microscopy. (A1-A3) On day 1, transfected seminiferous tubules showed dotted green fluorescence at low magnification (X10/0.45). Nuclei were counterstained with DAPI (blue staining) to reveal the structure of the seminiferous tubules. At the cellular level, fluorescence was detectable (B1-B3) in germ cells including Spermatogonia (Sg), Spermatocytes (Scytes) and round Spermatids (RStides), as well as (C1-C3) in Sertoli cells (SC). (D1-D3) On day 7, the GFP signal was lower at low magnification (X10/0.45) and detectable (E1-E3) only in Sertoli cells (40x/1.15 WI) (n=3). E4 is an enlargement of the red square in E3, allowing the cell type to be identified. Scale bars: 100 µm, 15 µm and 3 µm.

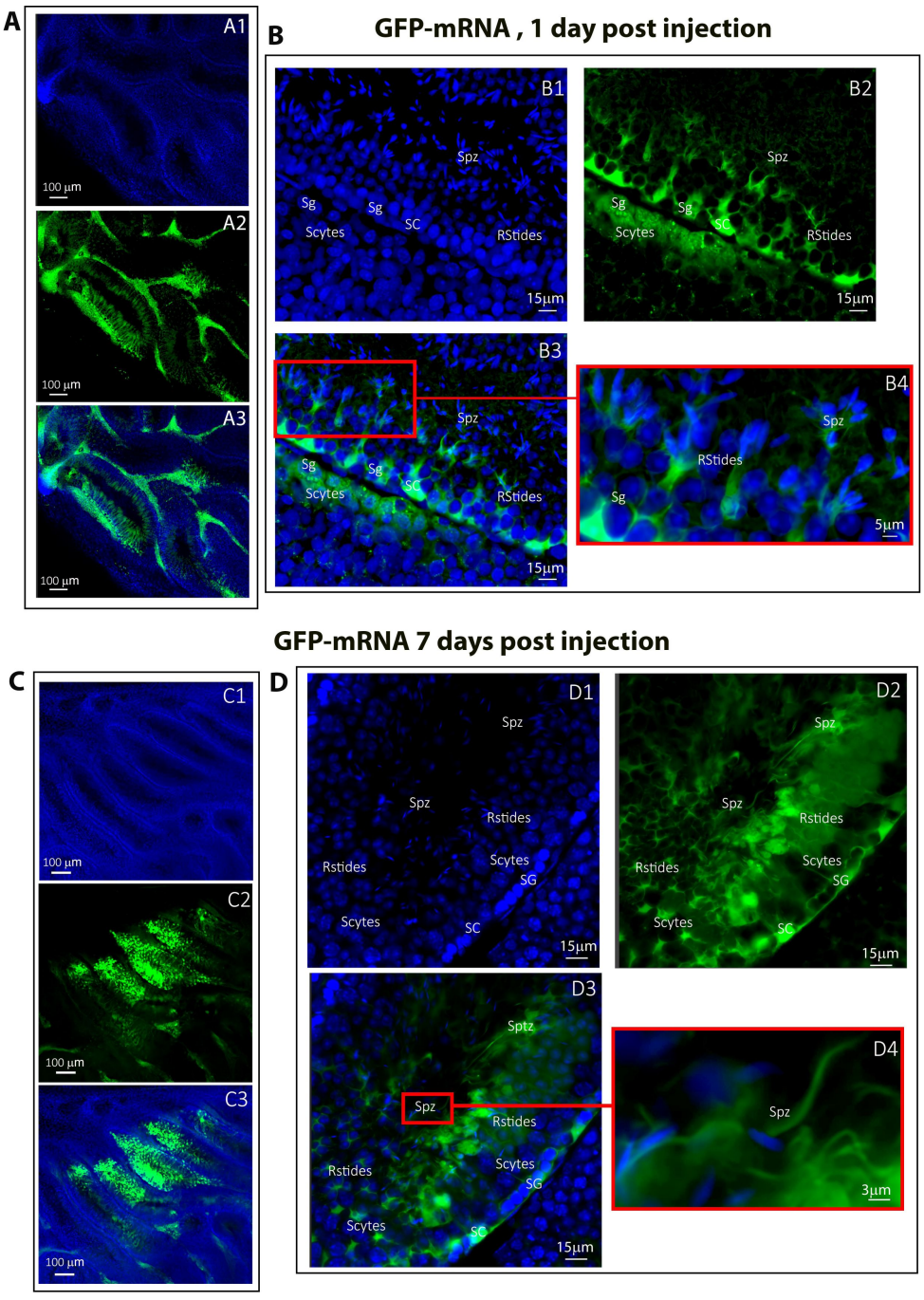

Figure 8.

Cellular expression of *GFP*-mRNA following *in vivo* injection/electroporation.

Testes were injected/electroporated with *GFP*-mRNA on day 0. On day 1 and day 7, whole testes were fixed and subjected to optical clearing. Cleared testes were observed by fluorescence microscopy. (A1-A3) On day 1, transfected seminiferous tubules showed strong broad-ranging green fluorescence at low magnification (X10/0.45). Nuclei were counterstained with DAPI (blue staining) to reveal the structure of the seminiferous tubule. At the cellular level, fluorescence was detectable in germ cells (B1-B3) including Spermatogonia (Sg), Spermatocytes (Scytes) and round Spermatids (RStides), Sperm cells (Spz) and Sertoli cells (SC). B4 is an enlargement of the red square in B3, allowing the cell types to be identified. (D1-D3) On day 7, the GFP signal remained strong at low magnification (X10/0.45) and (E1-E3) was still detectable in all germ cell types and Sertoli cells (40x/1.15 WI) (n=3). E4 is an enlargement of the red square in E3, showing that testicular sperm were also stained. Scale bars: 100 µm, 15 µm and 3 µm.

in the testes after injection and electroporation, we further challenged the method with another reporter protein – mCherry. We injected homemade naked mRNA coding for mCherry into the testes (**Fig supp 2BC**). As previously with *GFP*- mRNA, no testicular lesions were observed (**Fig supp 3** A1, B1, C1, D1, E1, F1). Assessment of the remanence of testicular expression of the mCherry fluorescent protein on days 0, 1, 7, 15, 21 and 28 post-injections revealed a strong red fluorescence from day 1 that remained detectable 15 days post-injection (**Fig supp3** B2, C2 and D2). At the cellular level, the fluorescent signal was detected in germ cells, including spermatogonia, spermatocytes, round spermatids, testicular sperm cells, and Sertoli cells on days 1 and 7 post-injection (**Fig supp 4**).

Finally, we compared the kinetics and levels of expression of the three different mRNA molecules, coding for mCherry, GFP and luciferase. By comparing the number of mice expressing *mCherry*-mRNA, *GFP*-mRNA and *luciferase*-mRNA fluorescence/luminescence over 21 days, we observed first that expression was detectable for all mRNAs on day 1, and second that the duration of expression was slightly different for the individual mRNAs. For instance, on day 15, 100%, 80% and 60% of mice injected with *GFP*-mRNA, *mcherry*-mRNA, and mRNA-*luciferase*, respectively presented fluorescence/bioluminescence and on day 21 100% of mice expressed GFP, whereas no signal was observed for mCherry or Luciferase (**Fig supp 5**).

7. Endogenous expression of ARMC2 in germ cells

Before attempting to rescue expression, we felt it was important to better characterize Armc2 expression in healthy germ cells, and in particular to study the timing of expression. By IF, we determined when ARMC2 protein translation started during spermatogenesis. For these experiments, dissociated cells from testes were observed to detect the presence of ARMC2 on different spermatogenic cells. ARMC2 was present only in the flagellum of elongated spermatids (**Fig 9A**). The specificity of the signal was validated using testicular cells from Armc2 KO mice, where no signal was observed on all spermatogenic cells (**Fig 9B**). In WT cells, no evidence of ARMC2 was found in earlier germ cell types like spermatogonia or spermatocytes (data not shown). These results suggest that the ARMC2 protein is expressed late during spermatogenesis.

8. Co-injection of *Armc2*-mRNA and *eGFP*-mRNA followed by electroporation is safe and induces green fluorescence in the seminiferous tubules

We next tested whether the injection and electroporation of two RNA molecules had any deleterious effects on testis anatomy and seminiferous tubule structure. We first verified the quality of *Armc2*-mRNA synthesis by transfecting HEK cells and performing Western blot (**Fig supp 2**). After this validation, we co-injected *Armc2*-mRNA and *eGFP*-mRNA into the left testes of mice, using the right testes as untreated controls. *eGFP*-mRNA was co-injected to verify and monitor transfection efficiency. The testes were observed under a binocular microscope at different times (3, 6, 10, 15, 21, 28 and 35 days) after electroporation to identify possible macroscopic degeneration of the seminiferous tubules. No morphological defects were observed in the testes co-injected with *Armc2*-mRNA and *eGFP*-mRNA. An example of control and injected testes from day 15 is presented in **Fig 10** A1, B1. The testes were also weighed at different times post-injection, and the weight ratios of injected testes to non-injected control testes were determined. For all time points, this ratio was close to 1 (**Fig 10 C**), confirming that the method and the mRNAs did not cause any injury at the organ level. Next, under blue light, the efficiency of the transfection was assessed by observing the GFP fluorescence at the surface of the testes. Obvious GFP fluorescence was observed on testes injected with *Armc2*-mRNA and *eGFP*-mRNA 2 weeks after injection (**Fig 10** B2), indicating that the naked mRNA was successfully transfected into testicular cells and remained present up to 2 weeks after surgery.

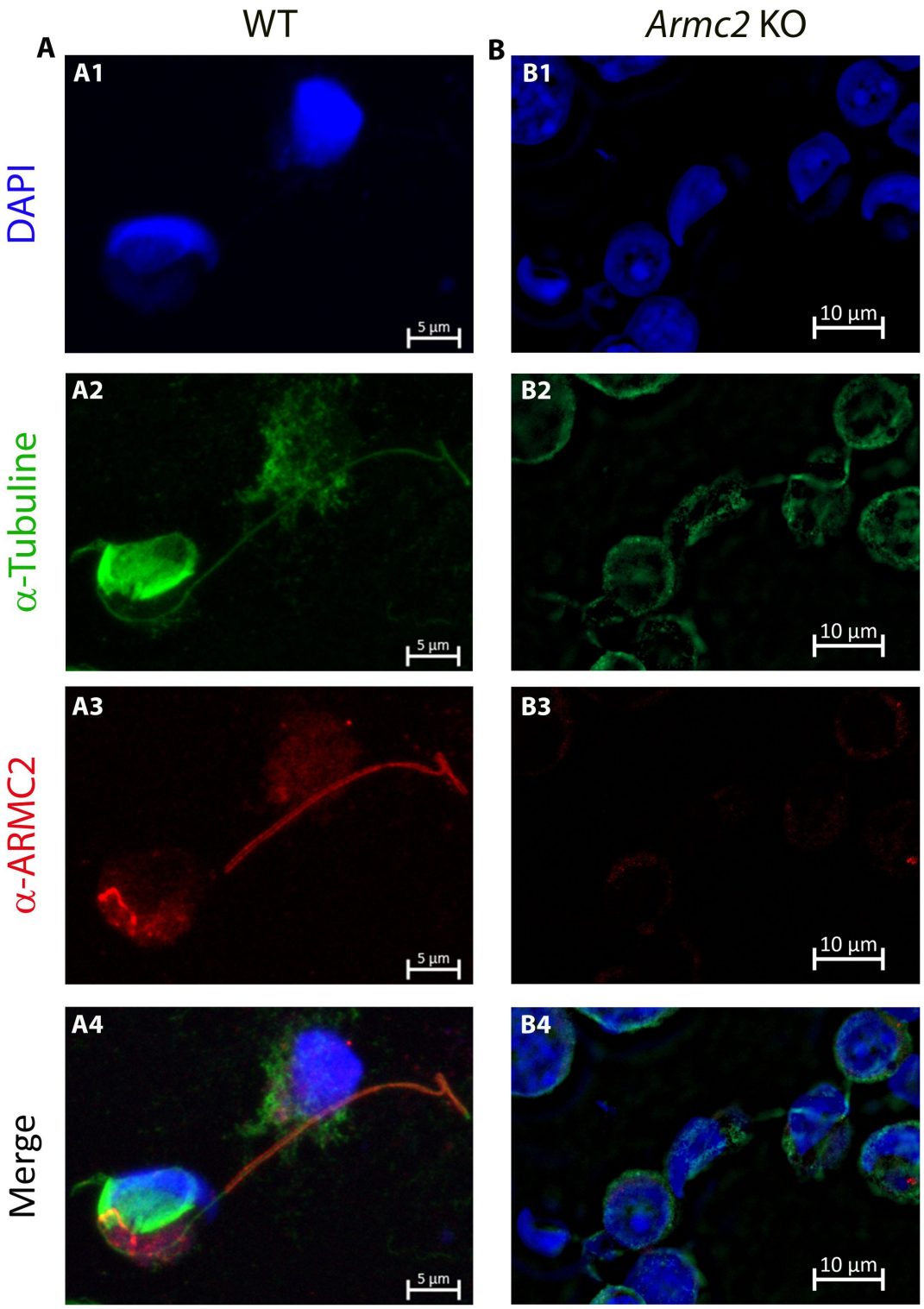

Figure 9.

ARMC2 localization in dissociated testicular cells observed by immunofluorescence.

Cells from WT and *Armc2* KO mice were stained with antibodies against ARMC2 (red signal) and tubulin (green signal). In WT mice, ARMC2 is located in the flagellum of spermatids. In KO mice, no ARMC2 signal (red fluorescence) was observed in any cells.

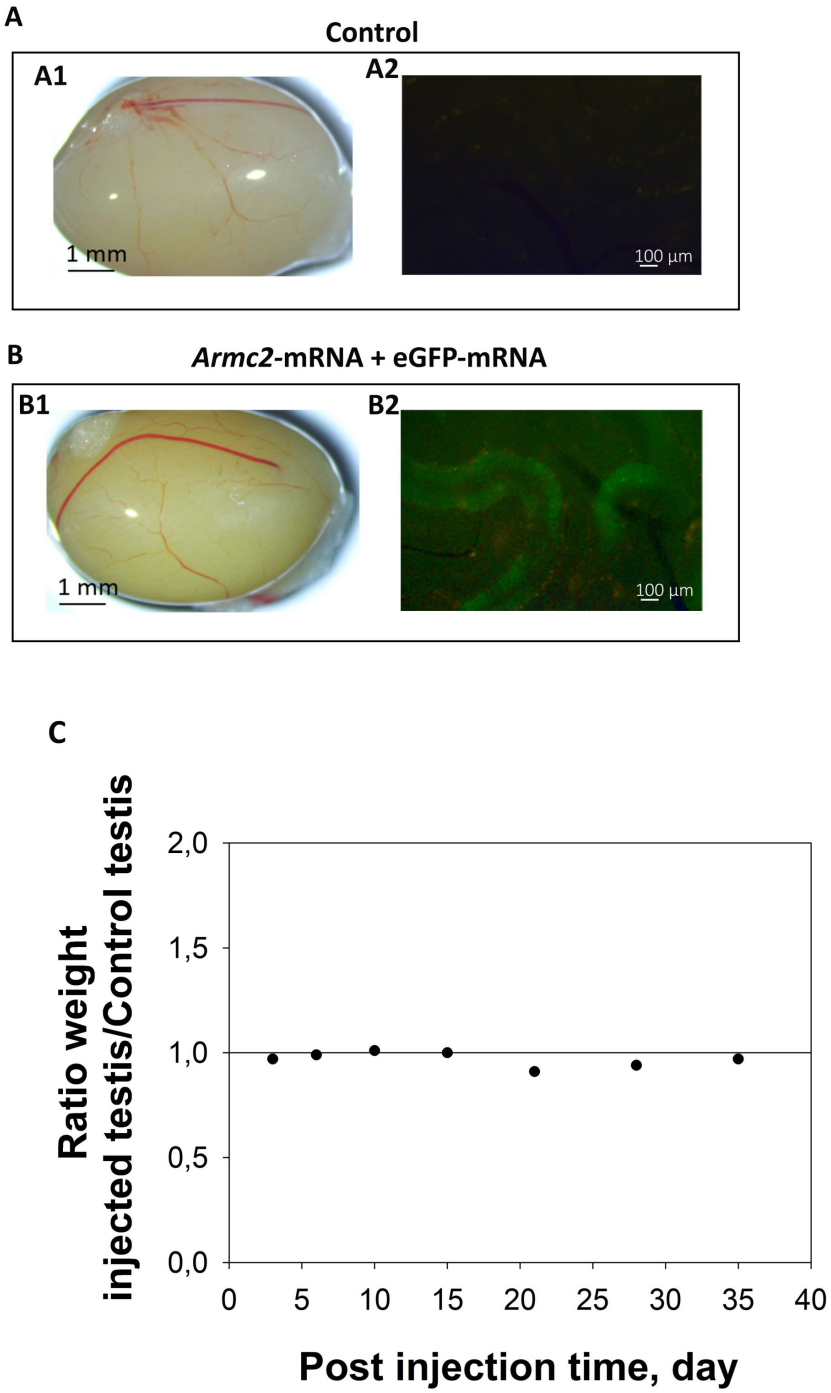

Figure 10.

***In vivo* co-injection of *Armc2*-mRNA and *eGFP*-mRNA followed by electroporation do not affect testes morphology and weight.**

Adult WT mouse testes were injected with a solution containing *Armc2*-mRNA and *eGFP*-mRNA. After injection, the testes were electroporated and mice were euthanized two weeks later. (A): Whole testis under white and blue lights on a fluorescence microscope (A1): control testes not injected or electroporated (A2): testes injected with *Armc2*-mRNA and *eGFP*-mRNA. *eGFP*-mRNA was co-injected to validate the transfection efficiency. (B): Ratio of injected/electroporated testis weights to control testis weights at several time points post-injection (3-, 6-, 10-, 15-, 21-, 28- and 35-days post-surgery). n= 1 mouse per time.

9. Motile sperm cells detected in *Armc2* KO mice following *Armc2*-mRNA injection and electroporation into testes

We then assessed whether the injection of *Armc2*-mRNA into the testes in *Armc2* KO mice restored sperm cell motility. We examined motility of sperm cells present in the caudal part of the epididymis at different times post-injection (3 to 35 days post-injection). For each condition, between 3 and 5 KO mice were used.

The *Armc2* KO model used is known to produce sperm cells with short and irregular flagella that are therefore immotile on day 0. No motile sperm were observed on days 3, 6, 10, 15 or 28 after surgery (**Fig 11 A**). However, motile sperm cells were found in the epididymis of some *Armc2* KO mice at 21- and 35-days post-treatment (**Fig 11 A**). Indeed, 1 in 3 mice had motile sperm cells at 21 days post-surgery, rising to 3/5 mice at 35 days post-injection. Nevertheless, the number of motile sperm cells observed remained low: 4.5% after 21 days and 6.15% after 35 days post-injection (**Fig 11 A**). Videos showing sperm motility in different conditions are available in the online material associated with this article (Videos 3 to 6).

After verifying motility, we looked at the morphology of the spermatozoa present in the cauda epididymis. Six days after injection of *Armc2*-mRNA, the cells detected were mostly round cells and abnormal spermatozoa with a short or coiled flagellum measuring between 7 and 20 µm. The same cell types were observed at 3-, 10-, 15- and 28-days post-surgery.

In contrast, the motile sperm detected on days 21 and 35 had a normal morphology with a long flagellum (greater than 100 µm) and a hook-shaped head (**Fig 11 B**).

Discussion

The challenge of treating male infertility remains to be addressed. Current assisted reproduction techniques (ARTs) are unable to treat all patients, and alternative strategies need to be developed to meet the legitimate desire to be a father. The aim of this study was to evaluate the potential of naked mRNA as a means to induce expression of exogenous proteins in male germ cells in a preclinical adult mouse model. Based on previous studies using electroporation, we investigated whether the combination of the injection of naked mRNA and in *vivo* electroporation could lead to efficient protein expression in spermatogenic cells. We chose to first study the efficiency of capped and poly-A-tailed mRNA coding for reporter proteins and compared results to those obtained with a non-integrative enhanced episomal vector plasmid. No EEV plasmid has ever been tested in the context of infertility treatment before this study.

Using an adult mouse model, we optimized the micro-injection and electroporation method described by Michaelis et al [7]. We show that the microinjection through the *rete testis* did not provide a homogenous distribution of the particles throughout the seminiferous tubules. Nevertheless, the seminiferous tubules remained intact, with no signal detected in the peritubular space. The peripheral expression observed was not due to the close vicinity of cells to the electrodes, but rather to a peripheral dispersal of the injected solution, as shown by the distribution of the fluorescent i-particles NIRFiP-180. Our results also showed that the combination of injection and electroporation is safe when electric pulses are carefully controlled. Using such a protocol, we were able to induce the expression of 3 reporter proteins, GFP, mCherry and luciferase in the testis by mRNA injection/electroporation. Based on whole testes fluorescence and, for the first time, *in vivo* bioluminescence imaging of testes, we characterized the kinetics of mRNA expression. Expression was observed to decrease rapidly after electroporation, with the total duration ranging from 15 to 21 days, depending on the molecule being expressed. Using whole

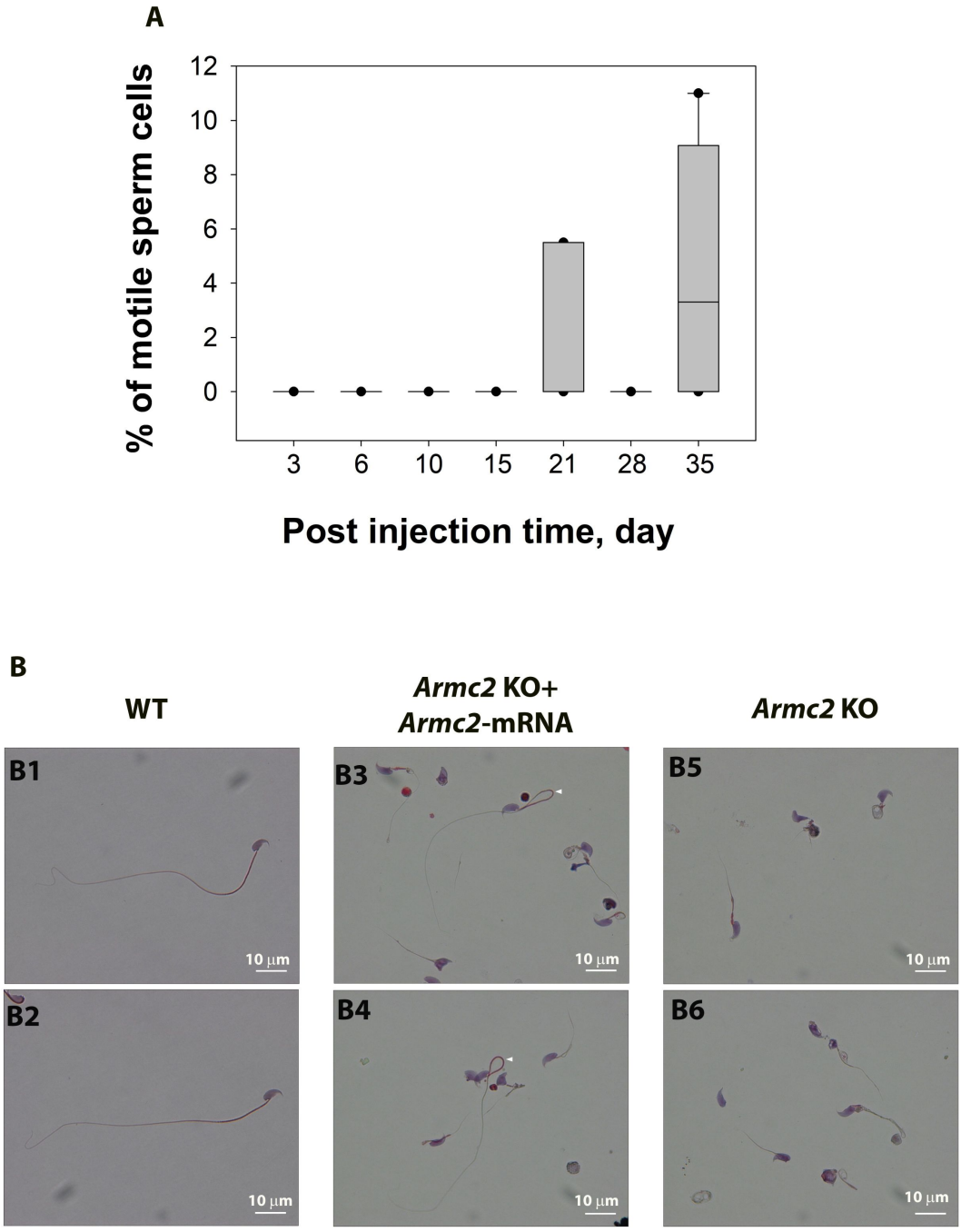

Figure 11.

Sperm motility is restored in *Armc2* KO mice at 21 and 35 days after injection and electroporation of *Armc2-mRNA*.

Adult *Armc2* KO mouse testes were injected with a solution containing *Armc2*-mRNA. After injection, the testes were electroporated. At different times (3-, 6-, 10-, 15-, 21-, 28-, and 35-days *post*-injection), sperm were extracted from the cauda epididymis of the injected testis, and the sample was then examined with a CASA system to identify the percentage of motile spermatozoa. n= 2 for 15 days, n= 3 for 3, 6 and 21 days, n= 4 for 10 days, and n= 5 for 28 and 35 days.
B) Morphology of sperm cells in *Armc2* KO mice injected or not with *Armc2*-mRNA. (B1-2): microscopic observation of epididymal sperm cells from a mature WT mouse. (B3-4): epididymal sperm cells from a mature *Armc2* KO mouse 35 days after injection/electroporation with *Armc2*-mRNA. (B5-6): epididymal sperm cells from a control *Armc2* KO male. Normal sperm cells were observed in the injected condition with *Armc2*-mRNA. (White arow) Scale bars:10 µm.

testicular optical clearing, the reporter proteins were synthetized from the injected mRNA in Sertoli cells, spermatogonia, spermatocytes, round spermatids, and spermatozoa from day 1, and were still detectable after 1 week.

When using the EEV vector, expression persisted for longer – up to 119 days – but with a lower yield of seminiferous tubule and cellular transfection. In particular, a lower level of transfection of germ cells was observed than with the mRNA, and after 1 week, only Sertoli cells remained transfected.

These results suggest that although EEV expression lasted longer, mRNAs, by targeting more efficiently male germ cells and allowing higher transfection yields of seminiferous tubules, could be a more effective and potent tool to express exogenous proteins in germ cells. By expressing a missing protein in the case of male infertility due to monogenic causes, it could be possible to restore failed spermatogenesis and thus to treat infertility.

ARMC2 is expressed in late spermatogenesis stages

Dissociated WT testicular cells contained ARMC2 in the flagellum of spermatids. No *Armc2* expression was detected in earlier germ cell type lineages like spermatogonia. These results suggest that the ARMC2 protein is expressed late during spermatogenesis, which explains why motile sperm were only found in the cauda epididymis from 3 weeks after injection in our treated mice. Indeed, full spermiogenesis (from round cell to sperm) takes around 15 days [17], and the journey across the epididymis lasts around 8 days, making a total of 3 weeks. Our results also confirm those recently published by Lechtreck et al. [18] from their study of the role of ARMC2 in the Intra-Flagellar Transport (IFT) of radial spokes in *Chlamydomonas.* Proteins are supplied to the flagellum by IFT trains, with some proteins binding directly to IFT train subcomplexes. This is the case, for example, for tubulin, which binds to the N-terminal domains of the central IFT-B proteins IFT74 and IFT81 [19]. In other cases, protein binding is mediated by adapters. For example, the placement of the Outer Dynein Arms (ODA) requires an adapter protein ODA16 [20]. Lechtreck et al. [18] suggested that the transport of the radial spokes along the flagellum involves ARMC2 acting as an IFT adapter [18]. The presence of ARMC2 in the flagella of elongating spermatid supports this hypothesis.

Exogenous *Armc2*-mRNA expression rescued the motility of oligo-astheno-teratozoospermic sperm

This is the first demonstration that proteins can be expressed in the testis following electroporation with capped and poly-A-tailed mRNA.

Our objective was to develop a new targeted therapeutic approach for infertility associated with monogenic defects. In this preclinical study, we tested the ability of mRNA to restore flagellar motility in a mouse model deficient for *Armc2* that displays an oligo-astheno-teratozoospermia .

Our results strongly suggest that the strategy is safe, as injection and electroporation of *Armc2*-mRNA or EEV-*Armc2* had no effect on testicular morphology or weight. More importantly, the technique was effective, with motile sperm cells found in *Armc2* KO epidydimal cauda 3 and 5 weeks after *Armc2*-mRNA injection. Naked mRNA injection/electroporation is therefore a promising method to treat infertility. In contrast, no motile spermatozoa were found after injection/electroporation of EEV-*Armc2*, confirming our previous results suggesting that this nucleic tool does not efficiently enter or transfect germ cells.

The method deployed here involved optimized, capped mRNA adapted for the expression of *Armc2*. The vector was injected via the rete testis into adult *Armc2* KO mice. The testes were then electroporated. The results obtained showed that the injected and electroporated testes had a

morphology and weight similar to the controls at all times after treatment, thus validating the safety of the method in this preclinical model of male infertility.

Although motile sperm cells were observed at 3- and 5-weeks after *Armc2*-mRNA injection into the epididymal cauda of *Armc2* KO mice, not all injected mice were efficiently treated. For instance, in a group of 5 mice littermates treated and euthanized at the same time (5 weeks post-injection), only 3 of the 5 had motile sperm cells. The absence of motile sperm at 5 weeks may be due to the type of spermatogenic cells transfected during the electroporation step. The transfected cells may differ between individuals, influenced by the injection and the position of the electrodes during electroporation. If the mRNA transfection takes place in a spermatogonia, it will take more than 6 weeks (including the time to cross the epididymis) before motile epididymal sperm cells emerge. This timeline could explain the absence of motile sperm in some littermates at 5 weeks.

Although we rescued the motility of oligo-astheno-teratozoospermic sperm, the transfection rate needs to be improved to obtain larger numbers of sperm cells. Indeed, our experiments did not provide enough motile sperm cells to carry out IVF or to allow natural mating. This low proportion could be explained by the mode of cell transfection. Nevertheless, ICSI with normal sperm could be implemented, increasing the overall safety of the technique.

Naked mRNA, a new therapeutic strategy to treat severe infertility

Non-obstructive Azoospermia (NOA) and severe oligozoospermia (SO) are the most severe disorders of spermatogenesis and are the most likely to be of genetic origin. NOA is defined by the complete absence of spermatozoa in the ejaculate. Approximately 10–15% of infertile men have azoospermia, and a further 15% have SO [21]. For patients with NOA, few clinical solutions are currently available. Generally, testicular sperm extraction is attempted to collect some spermatozoa from the seminiferous tubules, which can then be used for ICSI [22]. When no sperm are retrieved, intra-conjugal conception is impossible. Our results could also be applied to treat NOA, even if synthesis of the target protein does not persist throughout the whole spermatogenesis cycle. Indeed, it has been shown that spermatogenic proteins have a very low turnover [23] because synthesized proteins are stored in sperm organelles which remain stable until fertilization. Consequently, fertility rescue can probably be achieved even for proteins expressed earlier and involved in meiosis. Moreover, the presence of a few sperm in the ejaculate could be sufficient to obtain pups because with ICSI, only one sperm is required per oocyte. In other words, the persistent expression is not mandatory to treat infertility.

We used in this report electroporation to transfect the testicular cells. Although we injected 2/3 of the testes, the transfection is limited by the size of the electrodes which produce a restricted electric field. To increase the testicular transfection rate, encapsulation of mRNA into lipids nanoparticles could be used, as used for Covid vaccination [24]. During the writing of this manuscript, Dong team [25], used a self-amplifying RNA (saRNA) encapsulated in cholesterol-amino-phosphate derived lipid nanoparticle to restore spermatogenesis in infertile mice. They successfully restore the expression of the DNA Meiotic Recombinase 1 (DMC1) in *Dmc1* KO infertile mice by injecting a self-amplifying RNA-*Dmc1* in the testes. Dmc1 is 37 KDa protein implicated in the meiotic recombination during sperm meiosis [26–28]. Although this impressive article reported successful treatment of mouse infertility, a safety study should be carried out to validate such a method. Indeed, saRNA are genetically engineered replicons derived from self-replicating single-stranded RNA viruses [29]. They can be delivered encapsulated in lipid nanoparticles, or as a completely synthetic saRNA produced after the *in vitro* transcription. The saRNA contains the alphavirus replicase genes and encodes an RNA-dependent RNA polymerase (RdRP) complex which amplifies synthetic transcripts in situ and the target RNA sequence. The target RNA is expressed at high levels as a separate entity. As a result of their self-replicative activity, saRNAs can be delivered at lower concentrations than conventional mRNA to achieve comparable expression levels [30]. Moreover, saRNA constructs need to be condensed by a cationic carrier into a nanoparticle measuring ~100 nm to enable their uptake into target cells and protect the

saRNA from degradation [31]. Finally, saRNA will amplify the RNA without cellular regulation. For all these reasons, if such a strategy is to be pursued, a potential toxicity effect due to saRNA over expression must be investigated in the testes and progeny. Another difficulty with saRNA relates to the size of the molecular construct. saRNA sequences are large and complex. The length of the sequence RdRP is around 7 kilobases, which often makes the full length of saRNA more than 9 kilobases once the sequence for the protein of interest has been integrated [31]. Dong et al. [25] successfully used their saRNA construct to rescue spermatogenesis failure induced by the absence of the small protein Dmc1, but it may be more challenging with larger proteins such as the structural proteins involved in OAT, including the 98-kDa ARMC2 [13].

Our next step will be to assess whether encapsulating *Armc2*-mRNA in LNP-CAP could allow a larger number of germ cells to be transfected.

In conclusion, this paper presents the first *in vivo* testicular injection and electroporation of capped and poly A tailed mRNA, demonstrating that it is an efficient strategy to transfect male germ cells and that the duration of expression of the resulting proteins is compatible with restoring spermatogenesis. Our comprehensive study revealed mRNA to be more efficient than an episomal vector, despite longer-lived expression in male germ cells with EEV. The difference was linked to EEV achieving a lower rate of seminiferous tubule transfection and a shorter duration of expression in germ cells. Our results also showed for the first time that functional sperm motility can be restored in mice with an oligo-astheno-teratozoospermia phenotype using a technique combining injection and electroporation of capped and poly-A-tailed mRNA. The findings presented open new opportunities to develop efficient strategies to treat male infertility with monogenic causes.

Videos 1 and 2: 3D-microscopic reconstructions of face 1 and 2 of a testis injected with GFP-mRNA.

Video 3: CASA recording of WT epididymal sperm cells

Video 4: CASA recording of *Armc2* KO epididymal sperm cells

Videos 5 and6: CASA recordings of epididymal sperm cells from *Armc2* KO mice on day 21 and day 35, respectively, after injection/electroporation with *Armc2*-mRNA.

Acknowledgements

This work was supported by ANR-20-CE18-0007 grant to JE. This work was supported by the Fondation pour la Recherche Médicale, grant number « ECO202006011669 » to CV.

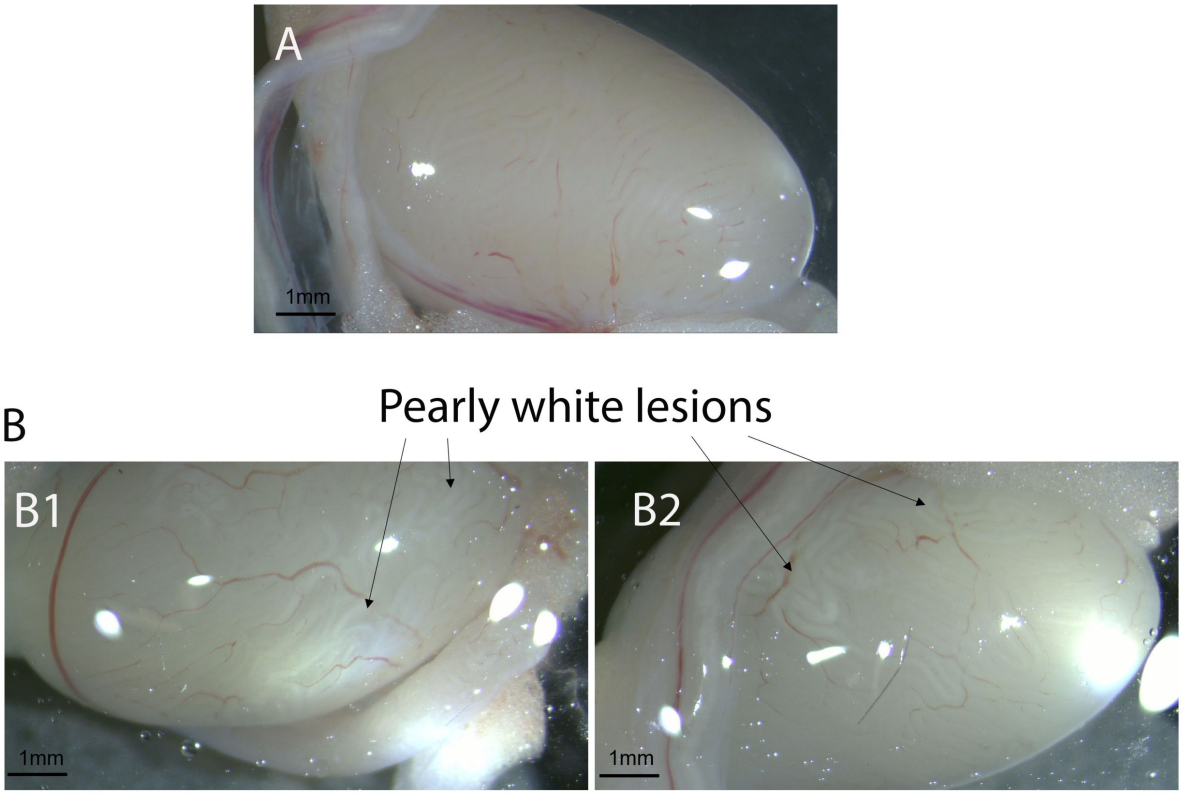

Fig supp 1

Damaged tubules observed by optical microscopy following overstimulation Adult mouse testes were *in vivo* injected and over electroporated using 10 square electric pulses to induce damage. (A) Control testis (no injection/electroporation). (B1-B2) Over electroporated testes showing damaged tubules as pearly white striations. Scale bars: 1 mm.

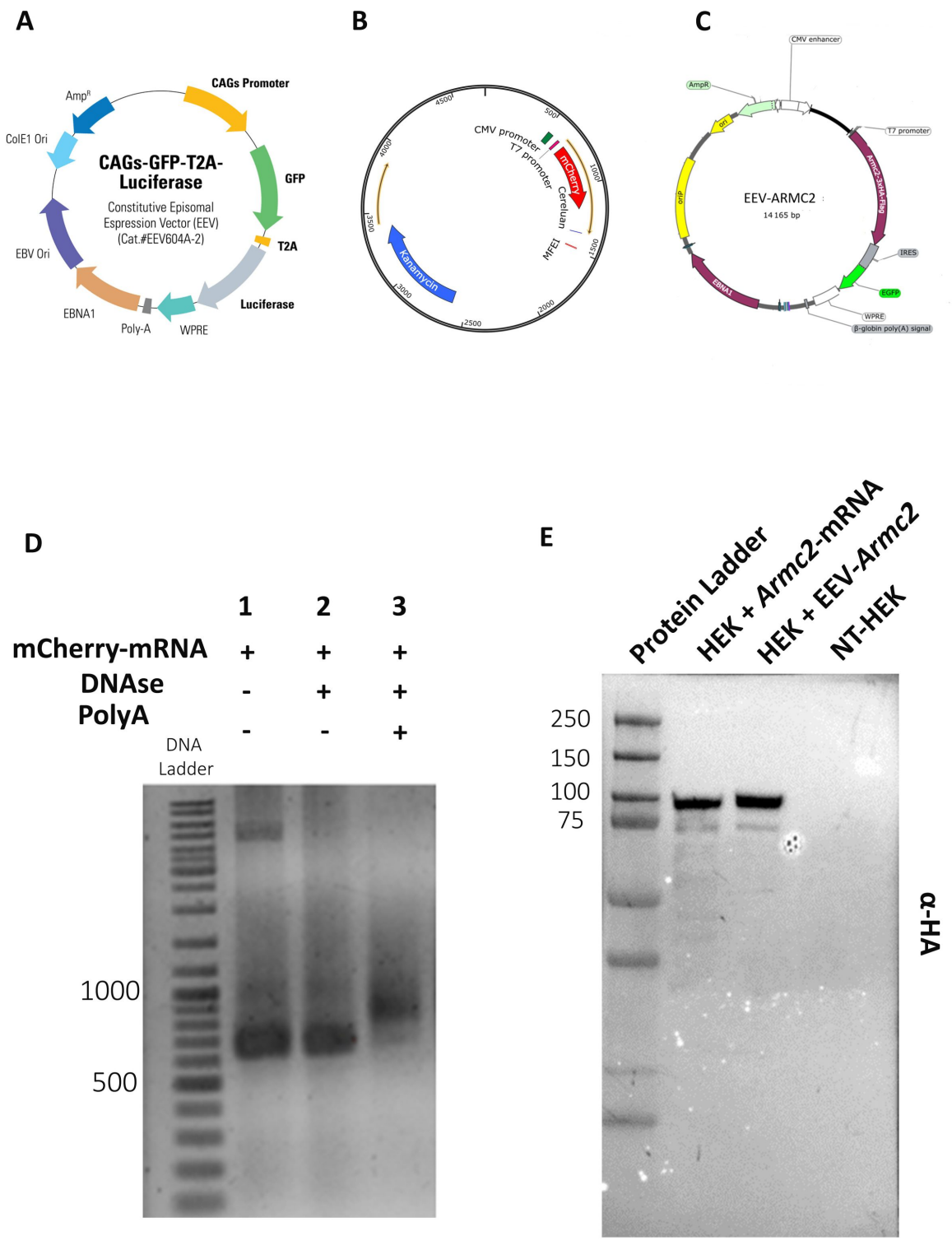

Fig supp 2

EEV and mRNA maps (A) EEV-plasmid map. The EEV-plasmid contains GFP, EVB ori, GFP, Luciferase, and EBNA sequences under the control of the GAGs promotor. (B) The mCherry plasmid contains the mCherry gene under the control of a T7 promotor. (C) The EEV-*Armc2* plasmid contains GFP, oriP, EBNA and *Armc2* sequences under the control of the CMV and T7 promotors. (D) *mcherry*-mRNA was synthetized as described in Material and Methods. It was validated by agarose gel electrophoresis: Lane 1: DNA size marker ladder (100 bp), lane 2: capped *mcherry*-mRNA (IVT product), lane 3: *mcherry*-mRNA after DNAse treatment. Capped and poly A tailed *mcherry*-mRNA migrated to the expected size of 876 bp. (E) Validation of *Armc2*-mRNA. HEK cells were transfected with *Armc2*-mRNA or EEV-*Armc2.* ARMC2 protein was detected by Western blot with an anti-HA primary antibody. The expected size for the ARMC2 protein is 98 kDa.

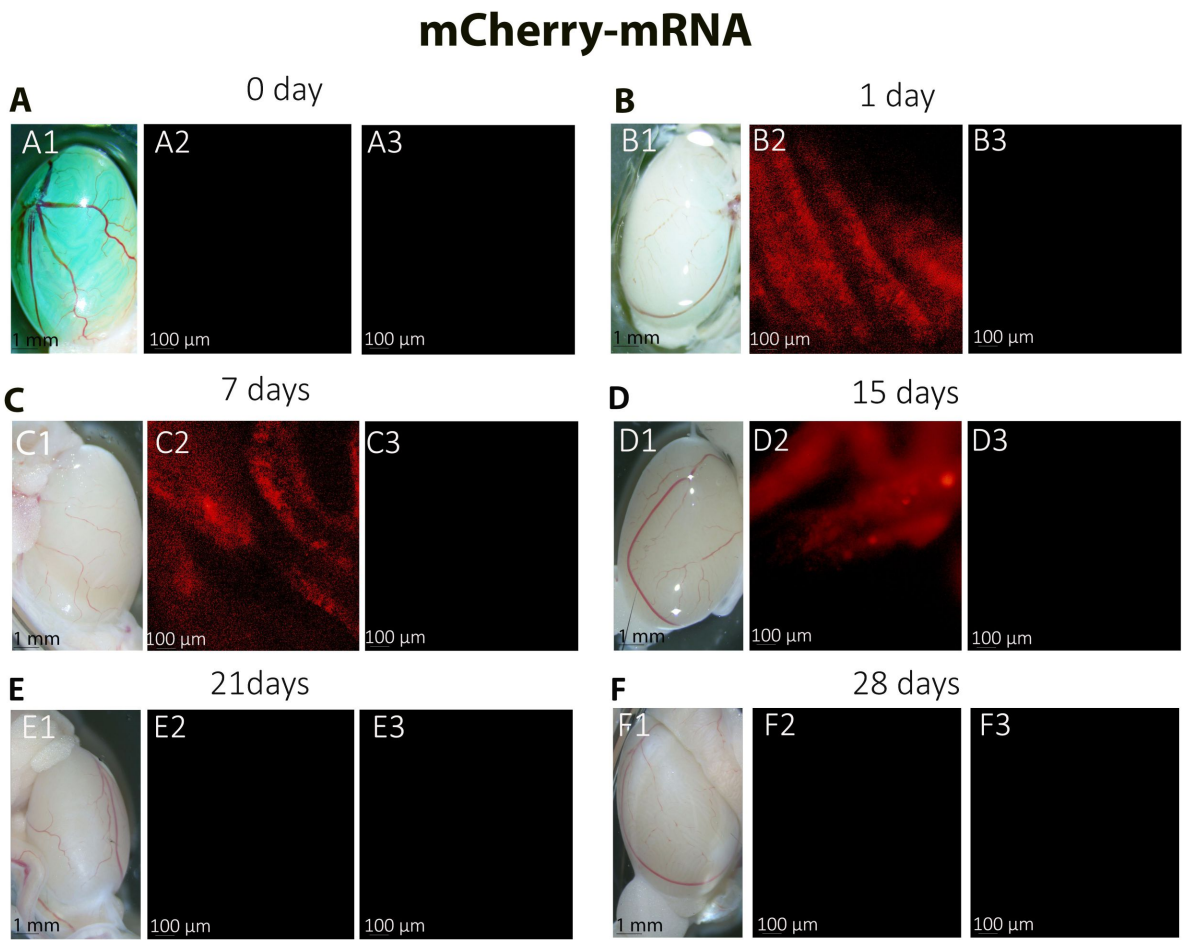

Fig supp 3

Testicular expression of *mcherry*-mRNA following in vivo electroporation (A1, B1, C1, D1, E1 and F1) Whole-mount testes on days 0, 1, 7, 14, 21, 28 after *in vivo* injection/ electroporation. (A2, B2, C2, D2, E2 and, F2) Using fluorescence microscopy, transfected testes from 12-week-old B6D2 mice express red mCherry fluorescence. mCherry was detected in a diffuse pattern throughout the seminiferous tubules from day 1 to day 15. (A3, B3, C3, D3, E3 and F3) images showing the absence of autofluorescence in non-transfected Control testes. (4X magnification). Scales bars: 1 mm and 100 µm.

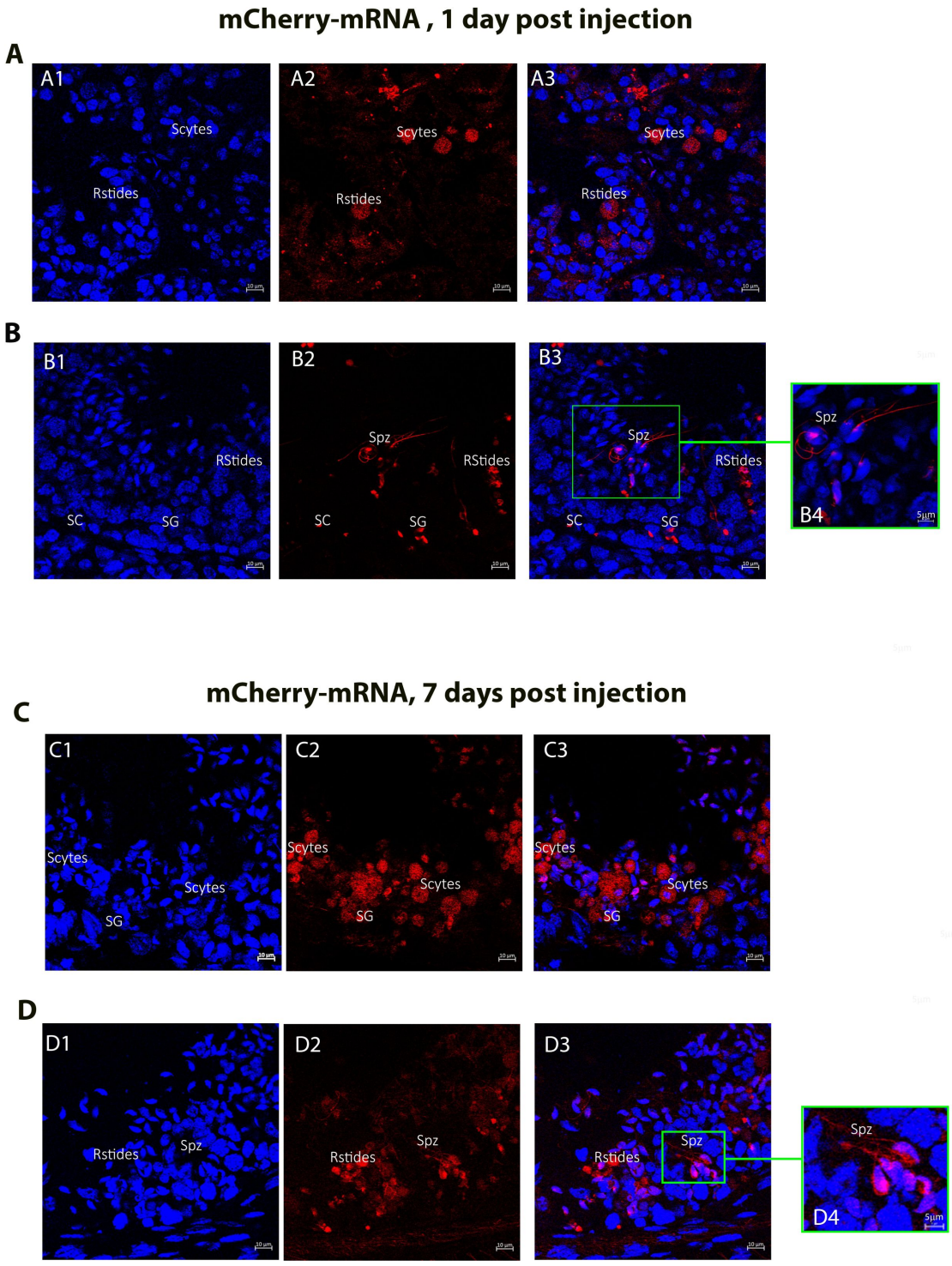

Fig supp 4

Cellular expression of *mcherry*-mRNA following in vivo injection/ electroporation.

Cross sections (20 µm) of mouse testes on day 1 (AB) and day 7 (CD) after in vivo injection and electroporation with *mcherry*-mRNA, observed under fluorescence microscopy. Red signals correspond to successfully transfected testicular tubular cells; nuclei were counterstained with DAPI (blue). At the cellular level, mCherry fluorescence was detectable in Sertoli cells (SC); Spermatogonia (SG); Spermatocytes (Scytes); round Spermatids (RStides), and Sperm cells (Spz); on day 1 and day 7 (Plan-Apochromat 63x/1,4 Oil, WD 190µm) (n=3). Scale bars: 10 µm and 5 mm.

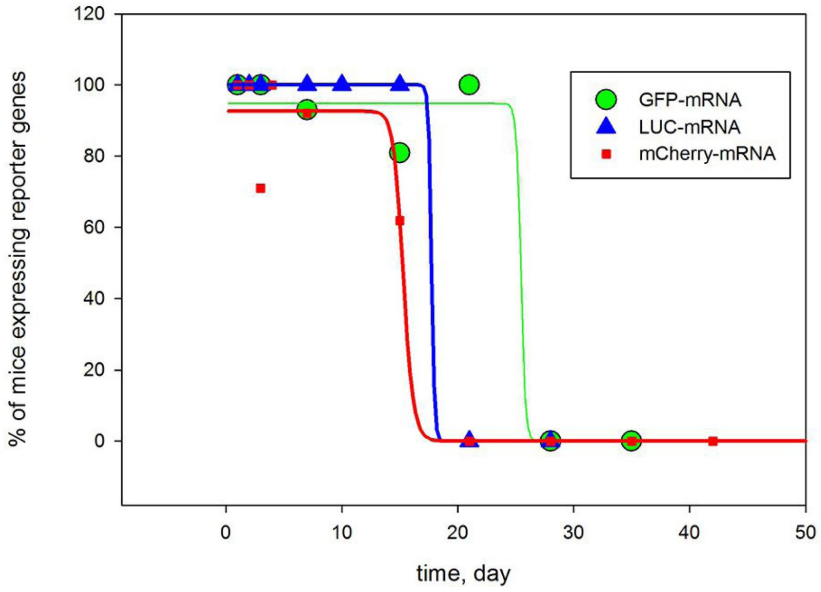

Fig supp 5

Decay over time of the number of mice exhibiting reporter gene expression following injection/electroporation of the three different mRNAs. Mice were injected on day 0 with *LUC*-mRNA, *GFP*-mRNA or *mcherry*-mRNA and the number of mice showing bioluminescence or fluorescence in the testis was counted at different time points. For *LUC*-mRNA n= 5 mice at each time point. For *mcherry*-mRNA n=3 on day 1; n=4 on day3; n=15 on day 7; n= 21 on day 15; n=15 on day 21; n= 5 on day 28; n=5 on day 35; and for *GFP*-mRNA n=3 on day 12; n=7 on day 2; n=7 on day 3; n=12 on day 7; n= 13 on day 15; n=10 on day 21 ; n= 9 on day 28; n=17 on day 35 and n=5 on day 42).

References

1. Boivin J., et al. (2007) **International estimates of infertility prevalence and treatment-seeking: potential need and demand for infertility medical care** *Hum Reprod* **22**:1506–12

2. Thonneau P., Spira A. (1991) **Prevalence of infertility: international data and problems of measurement** *Eur J Obstet Gynecol Reprod Biol* **38**:43–52

3. Uhlen M., et al. (2016) **Transcriptomics resources of human tissues and organs** *Mol Syst Biol* **12**

4. Davies M.J., et al. (2012) **Reproductive technologies and the risk of birth defects** *N Engl J Med* **366**:1803–13

5. Usmani A., et al. (2013) **A non-surgical approach for male germ cell mediated gene transmission through transgenesis** *Sci Rep* **3**

6. Raina A., et al. (2015) **Testis mediated gene transfer: in vitro transfection in goat testis by electroporation** *Gene* **554**:96–100

7. Michaelis M., Sobczak A., Weitzel J.M. (2014) **In vivo microinjection and electroporation of mouse testis** *J Vis Exp* **90**

8. Wang L., et al. (2022) **Testis electroporation coupled with autophagy inhibitor to treat non-obstructive azoospermia** *Mol Ther Nucleic Acids* **30**:451–464

9. Sadelain M., Papapetrou E.P., Bushman F.D. (2011) **Safe harbours for the integration of new DNA in the human genome** *Nat Rev Cancer* **12**:51–8

10. Ishii T. (2017) **Germ line genome editing in clinics: the approaches, objectives and global society** *Brief Funct Genomics* **16**:46–56

11. Duzgunes N., Cheung J., Konopka K. (2018) **Non-viral suicide gene therapy in cervical, oral and pharyngeal carcinoma cells with CMV-and EEV-plasmids** *J Gene Med* **20**

12. Hodin T.L., Najrana T., Yates J.L. (2013) **Efficient replication of Epstein-Barr virus-derived plasmids requires tethering by EBNA1 to host chromosomes** *J Virol* **87**:13020–8

13. Coutton C., et al. (2019) **Bi-allelic Mutations in ARMC2 Lead to Severe Astheno-Teratozoospermia Due to Sperm Flagellum Malformations in Humans and Mice** *Am J Hum Genet* **104**:331–340

14. **in Transforming and Scaling Up Health Professionals' Education and Training: World Health Organization Guidelines 2013. 2013: Geneva.**

15. Ruthig V.A., Lamb D.J. (2022) **Updates in Sertoli Cell-Mediated Signaling During Spermatogenesis and Advances in Restoring Sertoli Cell Function** *Front Endocrinol (Lausanne* **13**

16. de Boer P., de Vries M., Ramos L. (2015) **A mutation study of sperm head shape and motility in the mouse: lessons for the clinic** *Andrology* **3**:174–202

17. Ibtisham F., et al. (2017) **Progress and future prospect of in vitro spermatogenesis** *Oncotarget* **8**:66709–66727

18. Lechtreck K.F., et al. (2022) **Chlamydomonas ARMC2/PF27 is an obligate cargo adapter for intraflagellar transport of radial spokes** *Elife* **11**

19. Kubo T., et al. (2016) **Together, the IFT81 and IFT74 N-termini form the main module for intraflagellar transport of tubulin** *J Cell Sci* **129**:2106–19

20. Dai J., et al. (2018) **In vivo analysis of outer arm dynein transport reveals cargo-specific intraflagellar transport properties** *Mol Biol Cell* **29**:2553–2565

21. Cocuzza M., Alvarenga C., Pagani R. (2013) **The epidemiology and etiology of azoospermia** *Clinics (Sao Paulo* **68**:15–26

22. Ma Y., et al. (2019) **A risk prediction model of sperm retrieval failure with fine needle aspiration in males with non-obstructive azoospermia** *Hum Reprod* **34**:200–208

23. Hermann B.P., et al. (2018) **The Mammalian Spermatogenesis Single-Cell Transcriptome, from Spermatogonial Stem Cells to Spermatids** *Cell Rep* **25**:1650–1667

24. Schoenmaker L., et al. (2021) **mRNA-lipid nanoparticle COVID-19 vaccines: Structure and stability** *Int J Pharm* **601**

25. Du S., et al. (2023) **Cholesterol-Amino-Phosphate (CAP) Derived Lipid Nanoparticles for Delivery of Self-Amplifying RNA and Restoration of Spermatogenesis in Infertile Mice** *Adv Sci (Weinh* **10**

26. Takemoto K., et al. (2020) **Meiosis-Specific C19orf57/4930432K21Rik/BRME1 Modulates Localization of RAD51 and DMC1 to DSBs in Mouse Meiotic Recombination** *Cell Rep* **31**

27. Habu T., et al. (1996) **The mouse and human homologs of DMC1, the yeast meiosis-specific homologous recombination gene, have a common unique form of exon-skipped transcript in meiosis** *Nucleic Acids Res* **24**:470–7

28. Shinohara A., et al. (1997) **Saccharomyces cerevisiae recA homologues RAD51 and DMC1 have both distinct and overlapping roles in meiotic recombination** *Genes Cells* **2**:615–29

29. Tews B.A., Meyers G. (2017) **Self-Replicating RNA** *Methods Mol Biol* **1499**:15–35

30. Bloom K., van den Berg F., Arbuthnot P. (2021) **Self-amplifying RNA vaccines for infectious diseases** *Gene Ther* **28**:117–129

31. Kim J., et al. (2021) **Self-assembled mRNA vaccines** *Adv Drug Deliv Rev* **170**:83–112

Article and author information

Charline Vilpreux

Université Grenoble Alpes, Inserm U1209, CNRS UMR 5309, Team Genetic, Epigenetic and Therapies of infertility, Institute for Advanced Biosciences 38 000 Grenoble, France

Guillaume Martinez
Université Grenoble Alpes, Inserm U1209, CNRS UMR 5309, Team Genetic, Epigenetic and Therapies of infertility, Institute for Advanced Biosciences 38 000 Grenoble, France, UM de Génétique Chromosomique, Hôpital Couple-Enfant, CHU Grenoble Alpes, Grenoble, France
ORCID iD: 0000-0002-7572-9096

Magali Court
Université Grenoble Alpes, Inserm U1209, CNRS UMR 5309, Team Genetic, Epigenetic and Therapies of infertility, Institute for Advanced Biosciences 38 000 Grenoble, France

Florence Appaix
Université Grenoble Alpes, Inserm U1209, CNRS UMR 5309, plateforme microcell, Institute for Advanced Biosciences 38 000 Grenoble, France

Jean-Luc Duteyrat
Université Claude Bernard Lyon 1, CNRS UAR3444, Inserm US8, ENS de Lyon, SFR Biosciences, Lyon 69007, France
ORCID iD: 0000-0002-7126-8798

Maxime Henry
Université Grenoble Alpes, Inserm U1209, CNRS UMR 5309, plateforme Optimal, Institute for Advanced Biosciences 38 000 Grenoble, France

Julien Vollaire
Université Grenoble Alpes, Inserm U1209, CNRS UMR 5309, plateforme Optimal, Institute for Advanced Biosciences 38 000 Grenoble, France

Camille Ayad
Université Claude Bernard Lyon 1 – Laboratoire de Biologie Tissulaire et d'Ingénierie Thérapeutique, UMR 5305, Université Lyon 1, CNRS, IBCP, Lyon, France

Altan Yavz
Université Claude Bernard Lyon 1 – Laboratoire de Biologie Tissulaire et d'Ingénierie Thérapeutique, UMR 5305, Université Lyon 1, CNRS, IBCP, Lyon, France

Lisa De Macedo
Université Grenoble Alpes, Inserm U1209, CNRS UMR 5309, Team Genetic, Epigenetic and Therapies of infertility, Institute for Advanced Biosciences 38 000 Grenoble, France

Geneviève Chevalier
Université Grenoble Alpes, Inserm U1209, CNRS UMR 5309, Team Genetic, Epigenetic and Therapies of infertility, Institute for Advanced Biosciences 38 000 Grenoble, France

Emeline Lambert
Université Grenoble Alpes, Inserm U1209, CNRS UMR 5309, Team Genetic, Epigenetic and Therapies of infertility, Institute for Advanced Biosciences 38 000 Grenoble, France

Sekou Ahmed Conte
Université Grenoble Alpes, Inserm U1209, CNRS UMR 5309, Team Genetic, Epigenetic and Therapies of infertility, Institute for Advanced Biosciences 38 000 Grenoble, France

Elsa Giordani
Université Grenoble Alpes, Inserm U1209, CNRS UMR 5309, Team Genetic, Epigenetic and Therapies of infertility, Institute for Advanced Biosciences 38 000 Grenoble, France

Véronique Josserand
Université Grenoble Alpes, Inserm U1209, CNRS UMR 5309, plateforme Optimal, Institute for Advanced Biosciences 38 000 Grenoble, France

Jacques Brocard
Université Claude Bernard Lyon 1, CNRS UAR3444, Inserm US8, ENS de Lyon, SFR Biosciences, Lyon 69007, France
ORCID iD: 0000-0002-0752-5737

Coutton Charles
Université Grenoble Alpes, Inserm U1209, CNRS UMR 5309, Team Genetic, Epigenetic and Therapies of infertility, Institute for Advanced Biosciences 38 000 Grenoble, France, UM de Génétique Chromosomique, Hôpital Couple-Enfant, CHU Grenoble Alpes, Grenoble, France
ORCID iD: 0000-0002-8873-8098

Bernard Verrier
Université Claude Bernard Lyon 1 – Laboratoire de Biologie Tissulaire et d'Ingénierie Thérapeutique, UMR 5305, Université Lyon 1, CNRS, IBCP, Lyon, France

Pierre F. Ray
Université Grenoble Alpes, Inserm U1209, CNRS UMR 5309, Team Genetic, Epigenetic and Therapies of infertility, Institute for Advanced Biosciences 38 000 Grenoble, France, UM GI-DPI, CHU Grenoble Alpes, Grenoble, France
ORCID iD: 0000-0003-1544-7449

Corinne Loeuillet
Université Grenoble Alpes, Inserm U1209, CNRS UMR 5309, Team Genetic, Epigenetic and Therapies of infertility, Institute for Advanced Biosciences 38 000 Grenoble, France

Christophe Arnoult
Université Grenoble Alpes, Inserm U1209, CNRS UMR 5309, Team Genetic, Epigenetic and Therapies of infertility, Institute for Advanced Biosciences 38 000 Grenoble, France
ORCID iD: 0000-0002-3753-5901

Jessica Escoffier
Université Grenoble Alpes, Inserm U1209, CNRS UMR 5309, Team Genetic, Epigenetic and Therapies of infertility, Institute for Advanced Biosciences 38 000 Grenoble, France
For correspondence: jessica.escoffier@univ-grenoble-alpes.fr
ORCID iD: 0000-0001-8166-5845

Copyright

Editors

Reviewing Editor
Carmen Williams
National Institute of Environmental Health Sciences, Research Triangle Park, United States of America

Senior Editor
Wei Yan
University of California, Los Angeles, Torrance, United States of America

Reviewer #1 (Public Review):

The authors assess the effectiveness of electroporating mRNA into male germ cells to rescue the expression of proteins required for spermatogenesis progression in individuals where these proteins are mutated or depleted. To set up the methodology, they first evaluated the expression of reporter proteins in wild-type mice, which showed expression in germ cells for over two weeks. Then, they attempted to recover fertility in a model of late spermatogenesis arrest that produces immotile sperm. By electroporating the mutated protein, the authors recovered the motility of ~5% of the sperm, although the sperm regenerated was not able to produce offspring using IVF.

This is a comprehensive evaluation of the mRNA methodology with multiple strengths. First, the authors show that naked synthetic RNA, purchased from a commercial source or generated in the laboratory with simple methods, is enough to express exogenous proteins in testicular germ cells. The authors compared RNA to DNA electroporation and found that germ cells are efficiently electroporated with RNA, but not DNA. The differences between these constructs were evaluated using in vivo imaging to track the reporter signal in individual animals through time. To understand how the reporter proteins affect the results of the experiments, the authors used different reporters: two fluorescent (eGFP and mCherry) and one bioluminescent (Luciferase). Although they observed differences among reporters, in every case expression lasted for at least two weeks.

The authors used a relevant system to study the therapeutic potential of RNA electroporation. The ARMC2-deficient animals have impaired sperm motility phenotype that affects only the later stages of spermatogenesis. The authors showed that sperm motility was recovered to ~5%, which is remarkable due to the small fraction of germ cells electroporated with RNA with the current protocol. The 3D reconstruction of an electroporated testis using state-of-the-art methods to show the electroporated regions is compelling.

The main weakness of the manuscript is that although the authors manage to recover motility in a small fraction of the sperm population, it is unclear whether the increased sperm quality is substantial to improve assisted reproduction outcomes. The quality of the sperm was not systematically evaluated in the manuscript, with the endpoints being sperm morphology and sperm mobility.

Some key results, such as the 3D reconstruction of the testis and the recovery of sperm motility, are qualitative given the low replicate numbers or the small magnitude of the effects. The presentation of the sperm motility data could have been clearer as well. For example, on day 21 after Armc2-mRNA electroporation, only one animal out of the three tested showed increased sperm motility. However, it is unclear from Figure 11A what the percentage of sperm motility for this animal is since the graph shows a value of >5% and the reported aggregate motility is 4.5%. It would have been helpful to show all individual data points in Figure 11A.

The expression of the reporter genes is unambiguous; however, better figures could have been presented to show cell type specificity. The DAPI staining is diffused, and it is challenging to understand where the basement membranes of the tubules are. For example, in Figures 7B3 and 7E3, the spermatogonia seems to be in the middle of the seminiferous tubule. The imaging was better for Figure 8. Suboptimal staining appears to lead to mislabeling of some germ cell populations. For example, in Supplementary Figure 4A3, the round spermatid label appears to be labeling spermatocytes. Also, in some instances, the authors seem to be confusing, elongating spermatids with spermatozoa, such as in the case of Supplementary Figures 4D3 and D4.

The characterization of Armc2 expression could have been improved as well. The authors show a convincing expression of ARMC2 in a few spermatids/sperm using a combination of an anti-ARMC2 antibody and tubules derived from ARMC2 KO animals. At the minimum, one would have liked to see at least one whole tubule of a relevant stage.

Overall, the authors show that electroporating mRNA can improve spermatogenesis as demonstrated by the generation of motile sperm in the ARMC2 KO mouse model.

https://doi.org/10.7554/eLife.94514.1.sa2

Reviewer #2 (Public Review):

Summary:

Here, the authors inject naked mRNAs and plasmids into the rete testes of mice to express exogenous proteins - GFP and later ARMC2. This approach has been taken before, as noted in the Discussion to rescue Dmc1 KO infertility. While the concept is exciting, multiple concerns reduce reviewer enthusiasm.

Strengths:

The approach, while not necessarily novel, is timely and interesting.

Weaknesses:

Overall, the writing and text can be improved and standardized - as an example, in some places in vivo is italicized, in others it's not; gene names are italicized in some places, others not; some places have spaces between a number and the units, others not. This lack of attention to detail in the preparation of the manuscript is a significant concern to this reviewer - the presentation of the experimental details does cast some reasonable concern with how the experiments might have been done. While this may be unfair, it is all the reviewers have to judge. Multiple typographical and grammatical errors are present, and vague or misleading statements.

https://doi.org/10.7554/eLife.94514.1.sa1

Reviewer #3 (Public Review):

Summary:

The authors used a novel technique to treat male infertility. In a proof-of-concept study, the authors were able to rescue the phenotype of a knockout mouse model with immotile sperm using this technique. This could also be a promising treatment option for infertile men.

Strengths:

In their proof-of-concept study, the authors were able to show that the novel technique rescues the infertility phenotype in vivo.

Weaknesses:

Some minor weaknesses, especially in the discussion section, could be addressed to further improve the quality of the manuscript.

It is very convincing that the phenotype of Armc2 KO mice could (at least in part) be rescued by injection of Armc2 RNA. However, a central question remains about which testicular cell types have been targeted by the constructs. From the pictures presented in Figures 7 and 8, this issue is hard to assess. Given the more punctate staining of the DNA construct a targeting of Sertoli cells is more likely, whereas the more broader staining of seminiferous tubules using RNA constructs is talking toward germ cells.

Further, the staining for up to 119 days (Figure 5) would point toward an integration of the DNA construct into the genome of early germ cells such as spermatogonia and/or possibly to Sertoli cells. Given the expression after RNA transfection for up to 21 days (Figure 4) and the detection of motile sperm after 21 days (Figure 11), this would point to either round spermatids or spermatocytes.

These aspects need to be discussed more carefully (discussion section: lines 549-574).

It would also be very interesting to know in which testicular cell type Armc2 is endogenously expressed (lines 575-591).

https://doi.org/10.7554/eLife.94514.1.sa0